A Case Study of an Unusually Intense Atmospheric Gravity Wave

LANCE F. BOSART AND ANTON SEIMON

Department of Atmospheric Science, State University of New York at Albany, Albany, New York

(Manuscript received 6 August 1987, in final form 22 March 1988)

ABSTRACT

A remarkable long-lived, large-amplitude gravity wave in the Carolinas and Virginia on 27 February 1984 is investigated by means of a subsynoptic-scale case study. The wave was characterized by a minor wave of elevation followed by a sharp wave of depression with a period of 2–3 h, a horizontal wavelength of 100–150 km and surface pressure perturbation amplitudes of 3–14 mb. The wave propagated toward the east-southeast at 15 m s^{-1}, accelerating to more than 20 m s^{-1} after it crossed the Atlantic coast. Wave passage was accompanied by gusty surface easterly winds reaching 30 m s^{-1} and an abrupt termination of precipitation with the rapid surface pressure fall. The synoptic criteria identified by Uccellini and Koch as common to many cases of large amplitude gravity waves were present in this case.

Gravity waves were first detected across western Tennessee and northern Mississippi in a wake depression region to the rear of an advancing squall line. An amplifying wave emerged out of the wave packet across the southern Appalachians as the downstream squall line was most intense. The wave, once organized, amplified still further in the cold air damming region east of the Appalachian mountains and followed the back edge of the precipitation shield to the coast. Meanwhile, a second gravity wave formed just to the north of the primary wave in southeastern Kentucky around 1300 UTC 27 February. It propagated rapidly northeastward at ~30 m s^{-1} as a zone of enhanced pressure falls superimposed on a broader region of synoptic pressure falls.

Geostrophic adjustment appeared to play a prominent role in the organization and intensification of the primary gravity wave, whereas both shearing instability and geostrophic adjustment contributed to the genesis of the second wave. A particularly important aspect of this case was the juxtaposition of prominent jets in the upper and lower troposphere in the region of wave formation and amplification. The low-level jet carried a plume of warm, moist unstable air northward over cooler, stable boundary layer air and helped to trigger a line of active convection in northern Georgia. The gravity wave, which organized and intensified to the *rear* of the convective line, appeared as a prominent *wake depression* in the mean sea level isobaric pattern. Forced subsidence to the rear of the convective line in the presence of a deep, cold and stable boundary layer may have contributed to wave amplification. East of the mountains the prominent stable layer or wave duct was capped by a deep layer of weak stability and strong vertical wind shear containing a critical layer, conditions favorable for wave trapping and wave reflectance. Wave propagation and maintenance was in excellent agreement with the Lindzen and Tung ducted gravity wave model. Dissipation occurred as the wave approached and crossed the coastal front boundary.

1. Introduction

Nearly forty years ago, Brunk (1949) published a paper documenting the existence of a large-amplitude gravity wave in the central United States. The pressure pulsation could be tracked to the Atlantic coast as a wave of depression. Gusty easterly winds accompanied the wave passage together with pressure drops in excess of 5 mb at a number of locations. Brunk noted that there appeared to be a relationship between a line of severe convection and wave onset and propagation. Subsequent investigators such as Pothecary (1954), Wagner (1962), Ferguson (1967), Bosart and Cussen (1973), Eom (1975), Pecnick and Young (1984), Matsumoto and Okamura (1985), Bosart and Sanders (1986) and Lin and Goff (1987) have reported other examples of long-lived pressure pulses that appeared to be singular in nature. These papers have shown that the passage of a gravity wave can exert a significant impact on the mesoscale structure of precipitation and wind fields.

A common problem with all the aforementioned papers is that the authors experienced difficulty in pinning down wave genesis and maintenance mechanisms. Convection has been attributed as a source of wave formation (e.g., Ferguson 1967; Bosart and Cussen 1973; Einaudi et al. 1987 and Lin and Goff 1987) or as a result of gravity wave activity (Uccellini 1975; Stobie et al. 1983). Several papers (e.g., Matsumoto et al. 1967a,b; Miller and Sanders 1980; Matsumoto and Okamura 1985; Koch and Golus 1985) have considered convective motions and gravity waves as mutually dependent and difficult to separate processes. Frontogenetical processes, with or without convection, have also been discussed as possible sources of gravity

Corresponding author address: Dr. Lance F. Bosart, Dept. of Atmospheric Science ES-219, State University of New York, 1400 Washington Avenue, Albany, NY 12222.

waves (e.g., Ley and Peltier 1978; Bosart and Sanders 1986).

A comprehensive review of large-amplitude gravity waves and their possible origin and maintenance is given by Uccellini and Koch (1987). They have found a degree of commonality in the synoptic settings of such gravity wave cases previously described in the literature. Specifically, the waves tend to be characterized by a wave of depression or wave packets with periods of 1–4 h, horizontal wavelengths of 50–500 km and surface pressure perturbation oscillations of 0.5–5.0 mb. The waves tend to occur north of a surface frontal boundary and east or southeast of a jet streak that is propagating toward a downstream ridge in the pressure field aloft. Of the various source mechanisms for gravity waves described by Gossard and Hooke (1975), Uccellini and Koch (1987) remarked that vertical shear instability and geostrophic adjustment, particularly the latter, appeared to be important in their sample of 13 cases. The presence of a lower tropospheric inversion, mentioned by Lindzen and Tung (1976) as necessary to provide a wave duct to prevent rapid wave dispersion, is noted by Uccellini and Koch (1987) to be a feature of many of these cases.

A striking example of a large-amplitude gravity wave is shown by the barogram, precipitation and wind gust traces for Raleigh–Durham (RDU; key station locations shown in Fig. 2), North Carolina shown in Fig. 1. A spectacular station pressure plunge of ~14 mb in two stages occurs in ~40 min after 2000 UTC 27 February. The wave of depression is followed by an ~7 mb pressure increase back to a plateau and ambient pressure with a resumption of the synoptic-scale pressure fall by 0100 UTC 28 February. As will be shown later, the wave has a period of 2–3 h and a wavelength of 100–150 km. Heavy precipitation occurs *prior* to the pressure break and then tapers off rapidly and ceases as winds become gusty from the east with the pressure plunge. These weather characteristics have been cited by many of the aforementioned investigators in their case studies of other gravity wave events.

Figure 2 shows the chronology of three important mesoscale features that significantly affected the weather in much of the eastern United States on 27 February 1984. The large-amplitude gravity wave that crossed the RDU region in Fig. 1 had its origin in western Tennessee and northern Mississippi shortly after 0300 UTC 27 February. As will be demonstrated more completely later, the most noteworthy feature of the wave was its subsequent amplification as it crossed the Appalachian Mountains. The three hourly isochrones of wave-induced minimum pressure shown in Fig. 2 reveal that the wave moved generally eastward at nearly 15 m s^{-1}, accelerating to 20 m s^{-1} after 0000 UTC 28 February as it reached the Atlantic Ocean. Wave elongation in the north-northeast–south-southwest direction was observed across the mountains. Also displayed in Fig. 2 are the maximum surface wind gusts, most

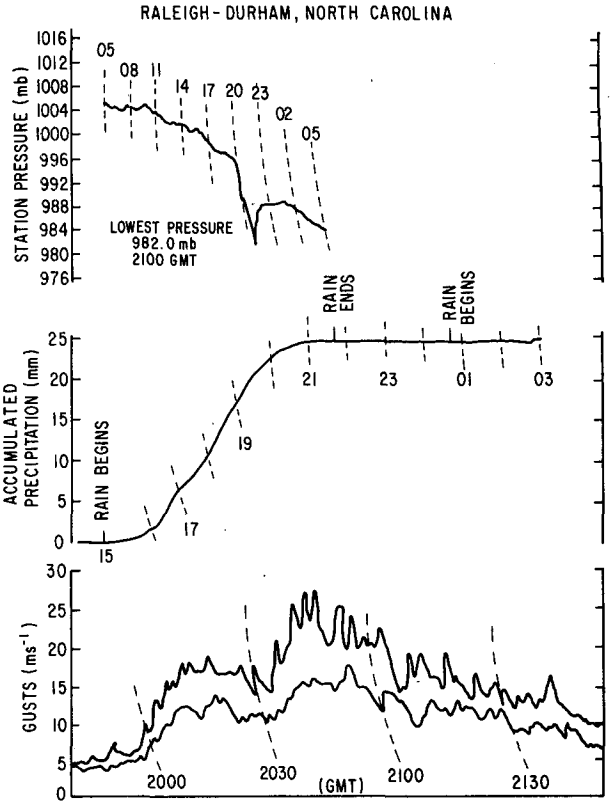

FIG. 1. Top: station pressure (mb), middle: accumulated precipitation (mm), bottom: smoothed envelope of wind gusts (m s^{-1}) for Raleigh–Durham, North Carolina, on 27–28 February 1984. Time in UTC.

of which occurred in conjunction with the wave passage. Across much of North Carolina, West Virginia, Virginia and the mountains of eastern Tennessee and southeastern Kentucky, damaging wind gusts of 25–35 m s^{-1} were reported.

A second feature of interest in Fig. 2 is the active squall line that entered western Mississippi by 0000 UTC 27 February. The line accelerated from 15 m s^{-1} to more than 20 m s^{-1} as it moved eastward, reaching peak intensity shortly before 1200 UTC across southern Georgia and the Florida panhandle. Subsequently, the squall line slowed to under 15 m s^{-1} as it weakened offshore. Note that the principal gravity wave was located in the *wake* of the squall line *and* to its north.

The third key mesoscale feature was a second gravity wave that appeared to form in southeastern Kentucky and extreme northeastern Tennessee shortly after 1200 UTC 27 February. It raced northeastward across West Virginia, Maryland and Pennsylvania (hourly isochrones shown in Fig. 2) at 30 m s^{-1} before losing its identity across extreme eastern Pennsylvania and northern New Jersey. Gusty easterly winds of under 15–20 m s^{-1} accompanied the passage of the wave.

The purpose of this paper is to document the struc-

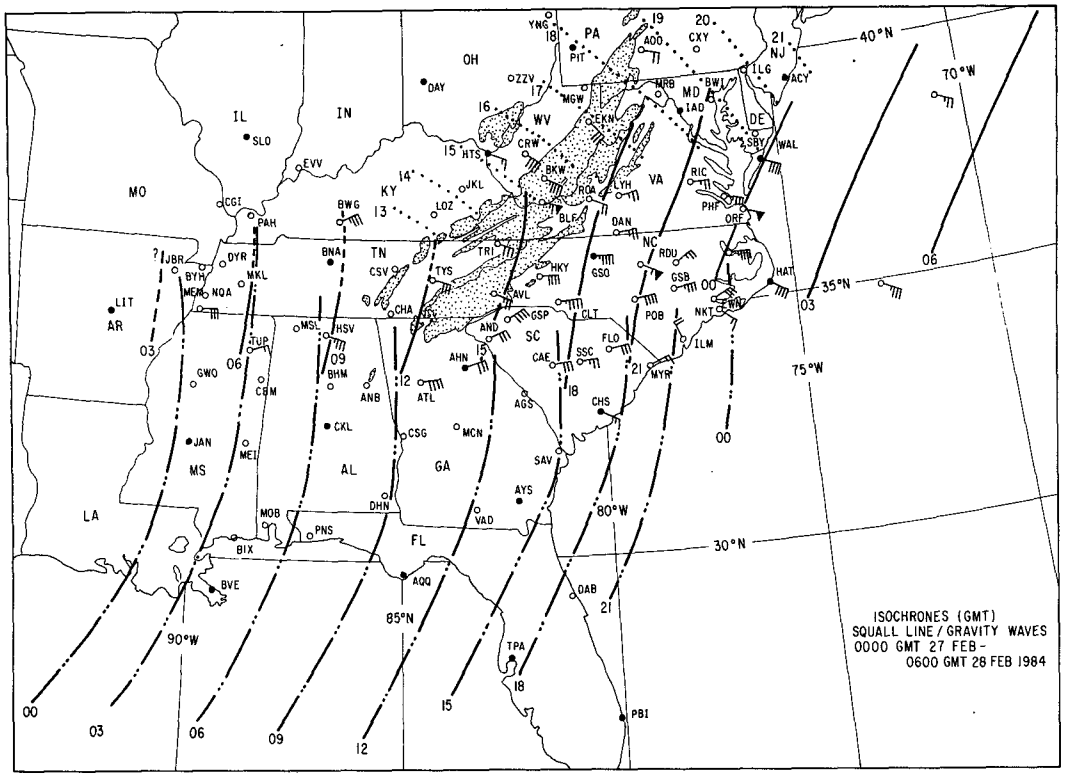

FIG. 2. Station locator map (solid circles denote locations of radiosonde stations) with terrain shown stippled for elevations > 600 m. Superposed three-hourly primary gravity wave isochrones (solid except dashed where ambiguous), squall line isochrones (long dash–double dot) and secondary gravity wave (dotted) hourly isochromes. Plotted winds (pennant, full barb and half barb denote 25, 5 and 2.5 m s^{-1}, respectively) represent peak reported wind speed with gravity wave passage. All times in UTC.

ture of the intense, singular long-lived gravity wave event. Emphasis will be placed upon the interaction of the wave with the larger scale flow and possible wave genesis and maintenance mechanisms. The paper is organized such that section 2 contains an overview of the synoptic-scale environment while the vertical structure is described in section 3. The subsynoptic-scale structure appears in section 4. Individual wave characteristics in the form of time sections and isochrone maps are presented in section 5. Section 6 describes the operational network radar-derived precipitation structure. Wave genesis and maintenance mechanisms are indicated in section 7, followed by conclusions and suggestions for further research in section 8.

2. Synoptic-scale structure

Surface sectional maps depicting sea-level isobars, surface isotherms and National Meteorological Center (NMC) frontal positions are displayed in Fig. 3 for 0000 and 1200 UTC 27 February. During this time a broad but modest cyclone moved slowly eastward across the lower Mississippi Valley. The presence of a warm, moist, unstable airflow from the Gulf of Mexico ensured a favorable environment for the aforementioned squall line to intensify overnight. Across the Carolinas and northeastern Georgia the surface pressure gradient strengthened and the baroclinity increased in conjunction with the onset of coastal frontogenesis and cold air damming. Note that both gravity waves formed within the cold air north of a surface frontal boundary.

Charts for 850 mb and 300 mb at 1200 UTC 27 February and 0000 UTC 28 February are presented in Fig. 4. An impressive low-level jet with peak winds of 35 m s^{-1} delineates a zone of intense 850 mb warm advection immediately in advance of the squall line at 1200 UTC. Farther west the remnant circulation center located over southwestern Arkansas reflects the original primary surface low. Incipient gravity wave formation before 0600 UTC and subsequent amplification after 1200 UTC takes place on the anticyclonic shear side of the low-level southerly jet. [At 0000 UTC 27 February the 850 mb low-level south-to-southeasterly jet runs from Boothville, Louisiana (BVE), to Jackson, Mississippi (JAN), to Little Rock, Arkansas (LIT), at a speed of 30 m s^{-1} to 20 m s^{-1}.] By 0000 UTC 28 February the 850 mb low-level jet has weakened somewhat and split into two pieces. The northern branch crosses the central Appalachians from east to west,

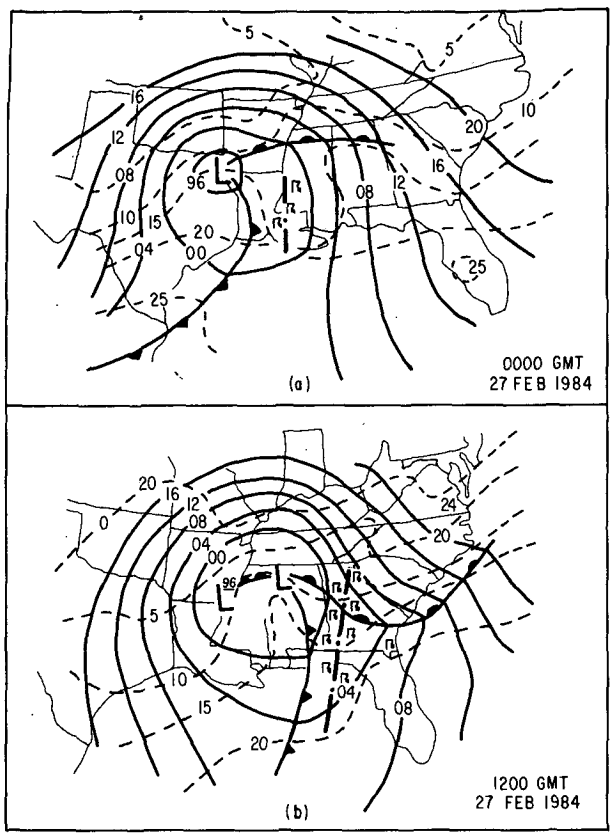

FIG. 3. Surface sectionals for (a) 0000 UTC and (b) 1200 UTC 27 February 1984. Sea level isobars (solid) every 4 mb and surface temperature (dashed) every 5°C with conventional frontal and weather symbols. Heavy dash–dot line denotes squall line position.

while there is evidence for a southern branch immediately ahead of the surface cold front. The main gravity wave, which now lies along the coast between Norfolk, Virginia (ORF), and Cape Hatteras, North Carolina (HAT), is still in a region of warm advection, but the strong anticyclonic shear is absent.

The corresponding 300 mb maps reveal that both gravity waves organized in a diffluent flow regime close to the downstream ridge and on the anticyclonic shear side of a jet (maximum winds > 60 m s^{-1}) upstream from Louisiana to central Tennessee. (Similarly, at 0000 27 February the 300 mb jet axis extended across northern Mexico, into southeastern Texas and then northward into central Arkansas. The maximum wind speeds in the jet over Texas were ~60 m s^{-1}.) By 0000 UTC 28 February there is increased meridional flow at 300 mb along the Appalachians, as the trough has deepened to the west while the ridge has held along the coast. Relative to the 300 mb jet, the gravity wave has remained on the anticyclonic shear side of the jet exit region and has moved eastward closer to the downstream ridge.

Satellite infrared cloud top temperatures derived from the McIDAS system in use at the State University of New York at Albany (SUNYA) are shown in Fig. 5 for selected time periods. At 0100 UTC 27 February there is a patch of cloud tops with temperatures < −60°C across Mississippi and eastern Louisiana as the squall line is getting organized. By 1200 UTC 27 February the squall line is close to maximum intensity, and there is a large area of cloud top temperatures < −60°C with extremes colder than −74°C. Gravity wave organization occurs in a region devoid of any characteristic cloud top signatures and *upstream* of the convective area.

At 1700 UTC 27 February the principal gravity wave is now well organized as it moves eastward across the Piedmont, whereas the weakening squall line to the east is associated with warmer cloud top temperatures than observed earlier across Georgia and the Carolinas. A narrow band of clouds with tops < −48°C that extends from extreme western North Carolina to extreme eastern Ohio could be followed for several hours in the half-hour infrared imagery when used in the loop mode on McIDAS. By 2000 UTC this band extends southward from central New York to central North Carolina. Of most interest, however, is the warming and thinning of the middle and high clouds immediately to the west of the surface position of the main gravity wave, which is now near peak intensity. Both the infrared and visible imagery clearly show the signal of the passage of the gravity wave in the middle and high cloud pattern. Pecnick and Young (1984) previously documented a case whereby thinning and dissipation of high cloudiness was observed in the satellite imagery *upstream* of the surface position of a long-lived large amplitude gravity wave. On the basis of a careful study of the satellite imagery using the McIDAS system, Pecnick and Young (1984) were able to deduce that the gravity wave filled the entire troposphere and tilted upshear in a manner consistent with the upper troposphere as a source for the gravity wave energy. They estimated adiabatic warming of 8°C at cirrus level with a maximum downward displacement of 900 m. An attempt to determine the vertical slope of the wave in the present case by similar means proved to be inconclusive, however, because of uncertainties in the interpretation of the satellite imagery.

3. Vertical structure

Vertical cross sections of the potential temperature (θ)/meridional wind component and the equivalent potential temperature (θ_e)/mixing ratio for 1200 UTC 27 February are displayed in Figs. 6a and 6b, respectively, along a Flint, Michigan (FNT), to Tampa, Florida (TPA), line. A southerly jet with maximum wind speed in excess of 40 m s^{-1} extends from 800 mb just north of Waycross, Georgia (AYS), to near 600 mb at Athens, Georgia (AHN). The southerly jet coincides with a tongue of moist unstable air. The northern limit of air with an upward decrease of θ_e is found

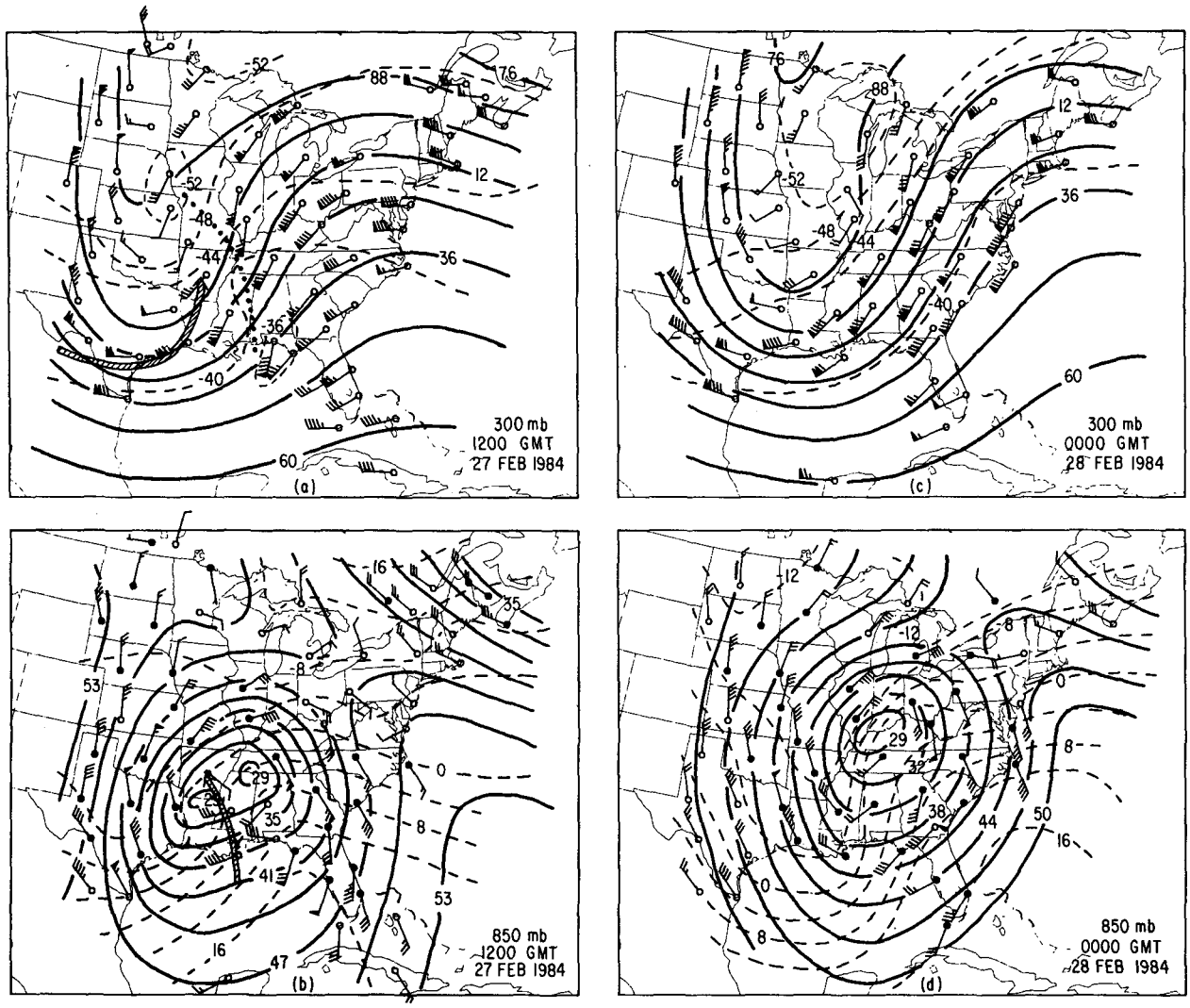

FIG. 4. Upper air sectional maps for (a) 300 mb and (b) 850 mb at 1200 UTC 27 February 1984 and for (c) 300 mb and (d) 850 mb at 0000 UTC 28 February 1984. Winds in m s^{-1} and temperatures in °C. Solid circles indicate a temperature–dew point temperature depression of ≤5°C. Plotting convention as in Figs. 2 and 3. The position of the 0000 UTC 27 February 300 mb ridge axis and jet axis is shown by the heavy dotted line and hatched arrow, respectively, in (a). The 850 mb low-level jet axis for the same time appears in (b) according to the same convention.

near AHN, where the 680–480 mb layer is conditionally unstable. South of AYS, deep conditional instability is indicated in the southerly airstream that is advancing northward ahead of the squall line. Clearly, this airmass can sustain elevated base thunderstorms across Georgia north of the surface frontal boundary in the presence of forced ascent. It is also apparent that the lower troposphere is dominated by multiple stable layers, the most prominent of which extends from above 600 mb at Dayton, Ohio (DAY), downward to below 700 mb at AHN. Above 500 mb the lapse rates are relatively steep.

The corresponding east–west cross sections from Oklahoma City, Oklahoma (OKC), to HAT are displayed in Figs. 7a, b. In the boundary layer the coldest air is confined to east of the Appalachian Mountains, where cold air damming is in progress, and to the southern Plains, where northerly flow is present in the wake of the surface cold front. A prominent low-level jet is centered near 800 mb at Nashville, Tennessee (BNA). This jet represents the northern anchor of the strong low-level flow from the Gulf of Mexico at 850 mb mentioned previously in Fig. 4b. The upper troposphere changes from strongly stable to weakly stable from the cyclonic to anticyclonic shear side of the upper-level jet above 300 mb. The lower troposphere is baroclinic throughout the cross section, with evidence for twin sloping stable layers between BNA and

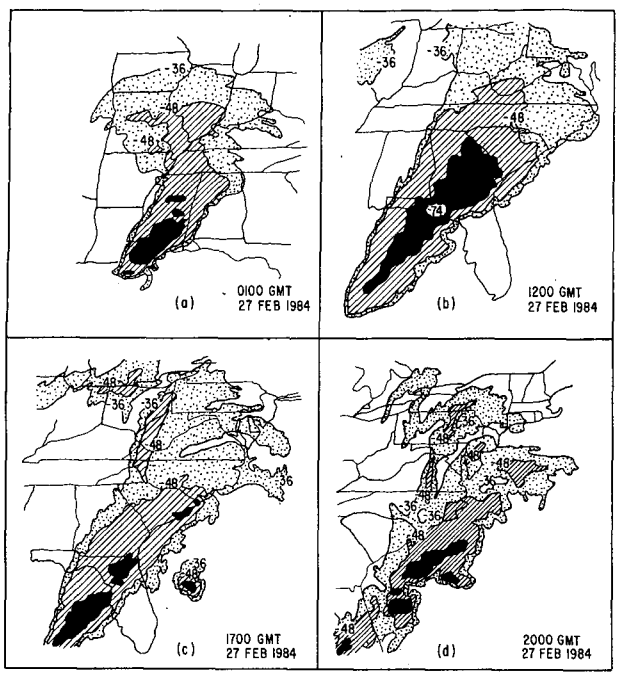

FIG. 5. Satellite infrared cloud top temperature (°C) contours for (a) 0100, (b) 1200, (c) 1700 and (d) 2000 UTC 27 February 1984. Contour thresholds at −36°C (dotted), −48°C (hatched), −60°C (solid) and −74°C (open).

Greensboro, North Carolina (GSO). The association of the low-level jet with a tube of conditionally unstable air (~775 mb to 525 mb) is relatively apparent at BNA, indicative of the potential for additional convection.

Figure 8 displays individual 1200 UTC 27 February soundings for AHN and Apalachicola, Florida (AQQ). Figure 9 displays the soundings for BNA and Centreville, Alabama (CKL). At both AHN and AQQ, the wind shear from the surface to 900 mb is very large (an aircraft hazard, as will be discussed later), but only at AQQ is there a prominent low-level jet. The time of the nominal balloon launch at AQQ was just after 1100 UTC, so the sounding is representative of conditions just ahead of the squall line, as a heavy thunderstorm is in progress at 1200 UTC. The nearly isothermal layer at AQQ below 900 mb is probably a reflection of marine conditions over the Gulf of Mexico. Comparison of the AHN and AQQ soundings reveals pronounced baroclinicity below 700 mb with the suggestion of convergence into the low-level jet.

The vertical wind profiles at BNA and CKL differ considerably. The strong low-level wind shear at BNA is a northward extension of the low-level jet sampled at AQQ. Note the rather large cyclonic vorticity and probable convergence implied by the observed winds below 800 mb at BNA and CKL. An important difference, however, is that the CKL sounding is sampling *post*-squall line air. The isothermal layer below 850 mb probably represents rain-cooled air, given the relatively light winds. In the 850–700 mb layer the weakly stable lapse rate and much drier air represent air that has subsided in the wake of the squall line. Of most interest, however, is the dramatic wind shear above 750 mb at CKL, with 600 mb winds exceeding 50 m s^{-1}. The corresponding stable layer at CKL (700–625 mb) and, to a lesser extent, at BNA (710–490 mb) reflects the extreme downstream end of a significant upper-level frontal zone that is propagating around the base of the amplifying upper-level trough (more fully described in O'Handley and Bosart (1989) that is in review). The dry air between 650 and 400 mb at BNA and CKL represents the signature of subsidence-induced warming and drying in the dry slot working around the base of the long-wave trough aloft.

The structure of the environment immediately upstream of the genesis region of the northern gravity wave and the rapid organization area of the southern gravity wave may be summarized as follows. 1) The airmass remains conditionally unstable for a 200–300 mb layer above relatively cool air in the boundary layer.

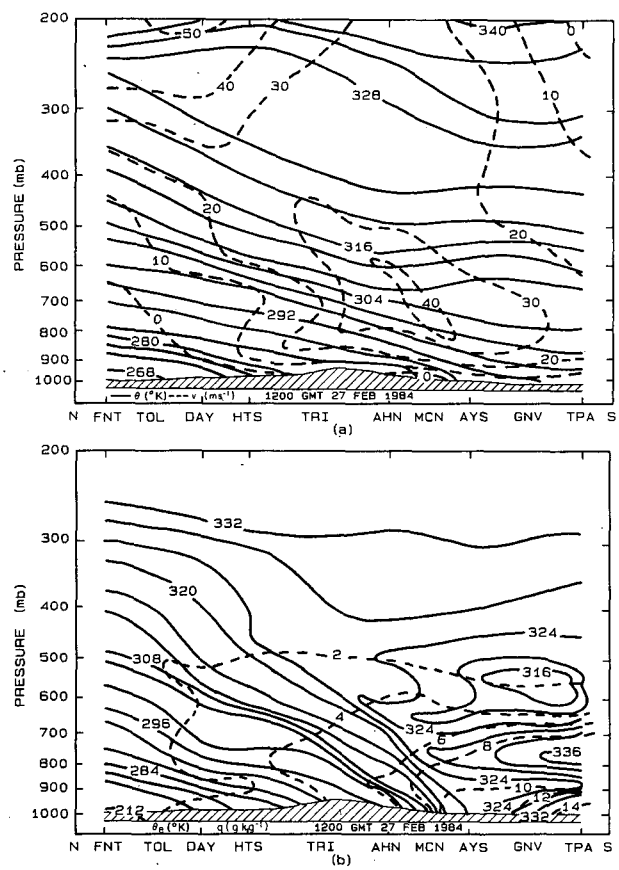

FIG. 6. North–south cross sections of (a) potential temperature (solid, °K) and north–south meridional wind component (dashed, m s^{-1}) and (b) equivalent potential temperature (solid, °K) and specific humidity (dashed, g kg^{-1}) along approximately 80°W for 1200 UTC 27 February 1984.

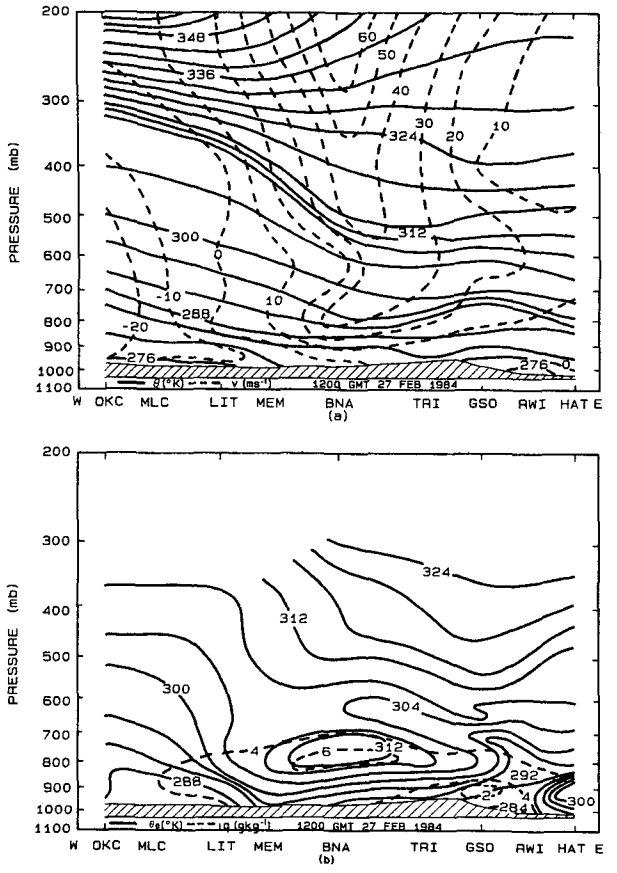

FIG. 7. As in Fig. 6 except for east–west section oriented along approximately 36°N.

Modest convection can then be triggered by forced ascent. 2) A stable layer, intensifying eastward, is present from the Tennessee Valley eastward to the Atlantic coast above mountain top level. It is capped by air of weak stability in the upper troposphere east of the jet axis aloft in central Tennessee. 3) At low levels a dome of cold air below mountain top level has formed east of the Appalachian Mountains. 4) Strong anticyclonic shear is found east of the low- and upper-level jets *and* east of the extreme downstream end of the upper-level frontal zone that has subsided to the 700–600 mb layer. 5) Strong vertical wind shear is present in both the lower and middle troposphere, as well as in the upper troposphere.

Soundings taken at Wallops Island, Virginia (WAL), and HAT for 0000 UTC 28 February are shown in Fig. 10. The WAL sounding, launched shortly after 2300 UTC 27 February, sampled conditions in the gusty easterly surface flow just prior to the passage of the gravity-wave-induced pressure minimum. At HAT, located on the warm side of the coastal front boundary, the boundary layer is well mixed along a moist adiabat just above the surface, and there is much less of a stable layer near 700 mb. The GSO soundings for 1200 UTC 27 February and 0000 UTC 28 February shown in Fig. 11 straddle the passage of the gravity wave. Notable aspects of the GSO soundings include 1) strong vertical wind shear, 2) a deep stable layer below 700 mb associated with cold air damming and 3) a warming and drying of the 725–575 mb layer, with the warming reaching almost to the surface rain-cooled air. Increased stabilization results.

4. Subsynoptic-scale structure

Figure 12a–i shows regional three-hourly surface maps for the 24 h period beginning 0000 UTC 27 February. In order to prepare the mean sea level pressure analyses, all available altimeter settings were extracted from a database of first and second order as well as from supplementary National Weather Service stations, military weather stations, offshore buoys and Coast Guard observations obtained from the National Climatic Data Center (NCDC). All available barograms (12 h and weekly) were manually digitized every 20 minutes to obtain a perturbation station pressure analysis. The mean sea level pressure analyses displayed in Fig. 12a–i represent the superposition of the synoptic and perturbation pressure fields in which extensive use of space to time conversion techniques was employed to produce a consistent set of maps. The decision to display the total pressure field (as opposed to the perturbation pressure field) was made on the basis of the observed large-amplitude wave signal in the present case, which makes it easier to view the interaction of synoptic and mesoscale pressure gradients on one map.

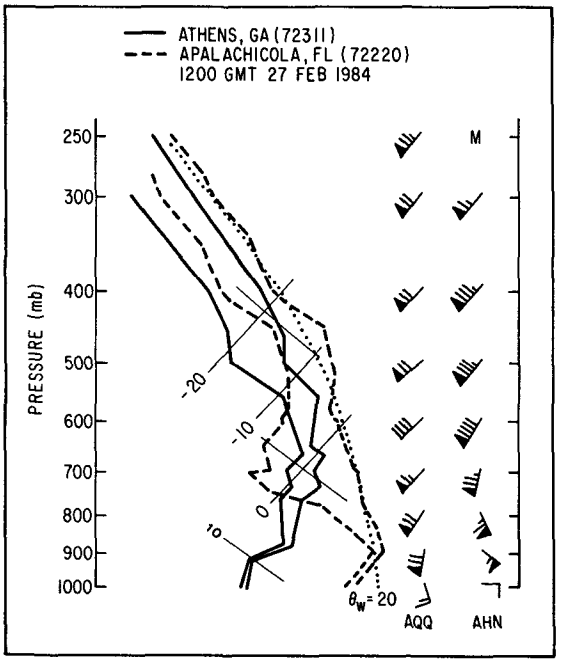

FIG. 8. Skew T–log$p$ format soundings for Athens, Georgia (solid), and Apalachicola, Florida (dashed), for 1200 UTC 27 February 1984. Plotted winds according to the format of Fig. 2.

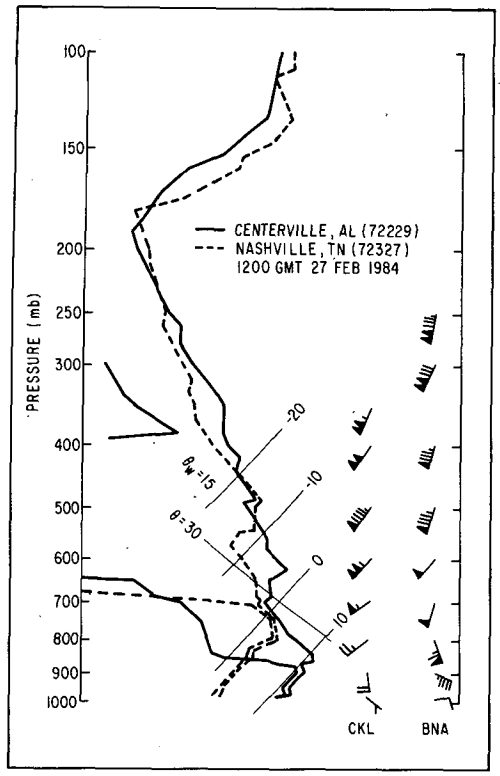

FIG. 9. As in Fig. 8 except for Centreville, Alabama (solid), and Nashville, Tennessee (dashed).

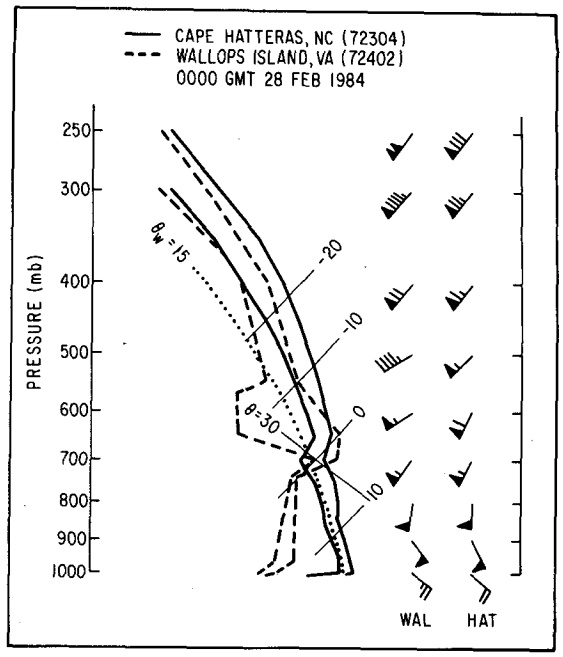

FIG. 10. As in Fig. 8 except for Cape Hatteras, North Carolina, (solid) and Wallops Island, Virginia (dashed), valid for 0000 UTC 28 February 1984.

Displayed in Fig. 12a is the regional map for 0000 UTC 27 February, which marks the time the squall line is organizing over Mississippi and southeastern Louisiana (in these figures only a subset of the actual observations available for analysis are plotted in order to preserve clarity). The primary low (994 mb) in northeastern Texas lies well upstream of the squall line. The northern half of the squall line lies in a baroclinic environment, but there is relatively little thermal contrast near the Gulf Coast. A large contrast in dewpoint temperature is found, however, with readings of <0°C in Alabama and Mississippi, near 5°C in the Florida panhandle, and in excess of 15°C in southeastern Louisiana and southern Mississippi immediately ahead of the squall line. Six-hour precipitation totals in excess of 50 mm over portions of Louisiana and Mississippi are reported with the squall line. To the rear of the squall line there is the well-known wake high, especially across eastern Arkansas, followed by a return to cyclonic curvature and lowered pressure in the vicinity of the primary low center. Barograms at this time (not shown) reveal the characteristic pre-squall line pressure plunge and an abrupt rise with wind shift to the west followed by a more gentle fall. The barograms also reveal numerous pressure oscillations of amplitude ± 1 mb in advance of the squall line.

By 0300 UTC (Fig. 12b) there is abundant evidence for a rapidly moving gravity wave (phase velocity ~ 25–30 m s^{-1}) in central Alabama. This wave, located at the eastern edge of the precipitation shield, is characterized by a pressure plunge of 2–3 mb (wave of depression followed by a 1–2 mb pressure rise) on a

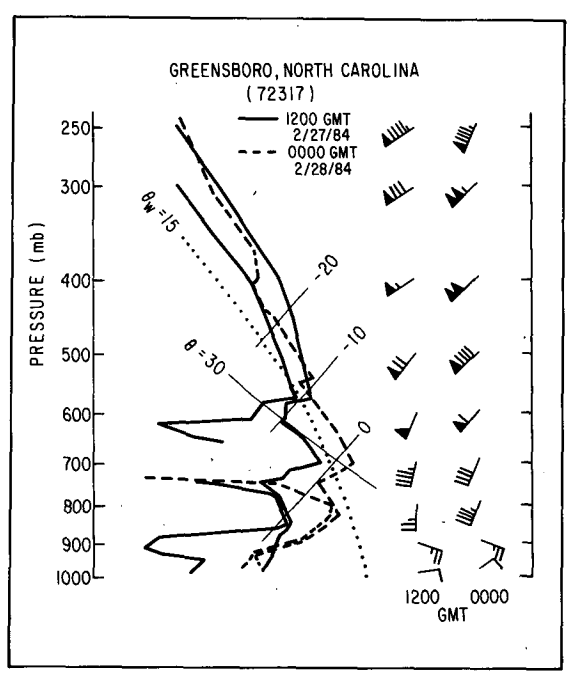

FIG. 11. As in Fig. 8 except for Greensboro, North Carolina, valid for 1200 UTC (solid) 27 February and 0000 UTC (dashed) 28 February 1984.

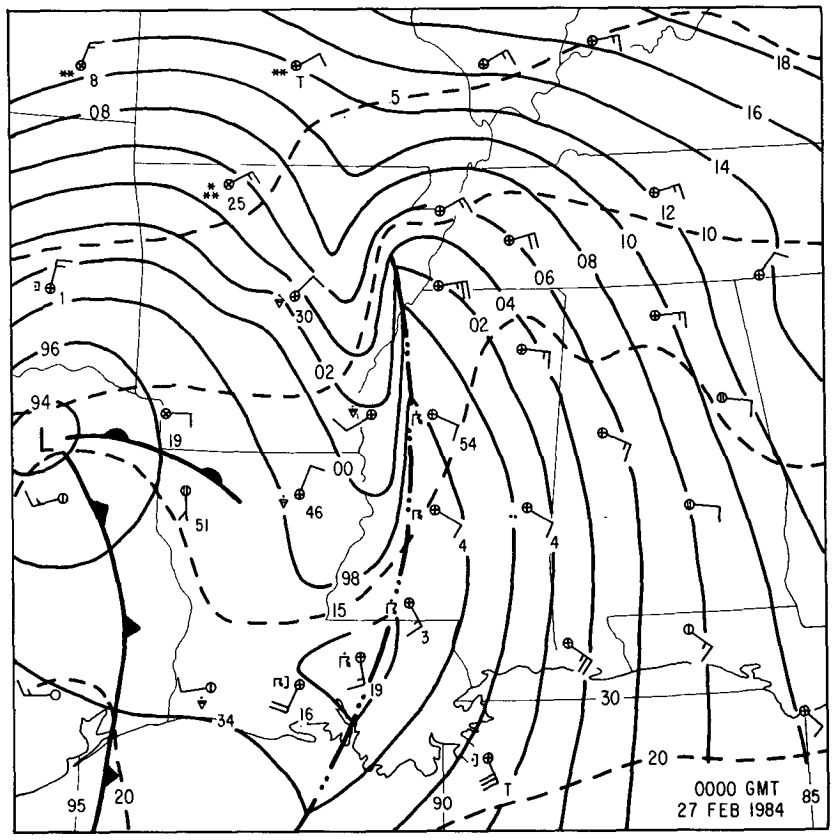

FIG. 12a. Surface sectional maps of sea level pressure (solid, mb) and temperature (dashed, °C) valid at 0000 UTC 27 February 1984. Selected winds plotted according to the format of Fig. 2. Conventional notation for weather depiction and frontal boundaries. Squall line positions indicated by long dash–double dot lines. Location of organizing gravity wave shown by heavy dotted line prior to 1500 UTC. Accumulated 6-h precipitation amounts (mm) appear to the lower right of a station at the conventional reporting times.

time scale of 30–60 minutes. The winds are gusty ($\sim$10–12 m s^{-1}) from the east during the period of rapid pressure fall and remain from the east, albeit slightly less strong, in the wake of the wave. The wave appears to become organized immediately ahead of the squall line around 0100 UTC, whereupon it outraces the squall line, weakens, and is for all purposes lost from the pressure perturbation analysis (not shown) by 0600 UTC. An area of minor surface pressure oscillations ($\sim \pm 1$ mb) is approaching the Blytheville, Arkansas (BYH),-Memphis, Tennessee (MEM), area.

By 0600 UTC (Fig. 12c) the strengthening squall line has reached western Alabama. Six-hour rainfall totals of 30–45 mm are common over a wide area. As the squall line propagates eastward at 15–16 m s^{-1} *through* the baroclinic zone, the largest pressure rises are found behind the line where the surface air is coolest and the radar-determined convective elements (discussed more fully in section 6) are comparatively less vigorous. The first real evidence for the developing principal gravity wave is now seen in the wake trough structure across extreme northern Mississippi and extreme southwestern Tennessee. Farther south an east–west oriented warm frontal boundary across southern Mississippi separates a region of light easterly flow in the wake of the squall line from warmer and more moist southwesterly flow of Gulf origin.

A distinguishing feature of the 0900 UTC map (Fig. 12d) is the eastward acceleration of the squall line to $\sim$18–20 m s^{-1} and the increasing baroclinity across central Georgia as cold air damming begins. Of most interest, however, is that the trailing pressure ridge (rain-cooled downdraft air) to the rear of the northern half of the squall line is becoming squeezed and more accentuated by the continued development of a wake pressure trough in extreme northern Alabama and central Tennessee. Separate troughing is also accentuated over eastern Tennessee in the downslope easterly flow from the high mountains.

By 1200 UTC (Fig. 12e and compare with Fig. 2) the squall line, which is now close to maximum intensity from Georgia southward into the Gulf of Mexico (recall Fig. 5), continues to propagate eastward *ahead*

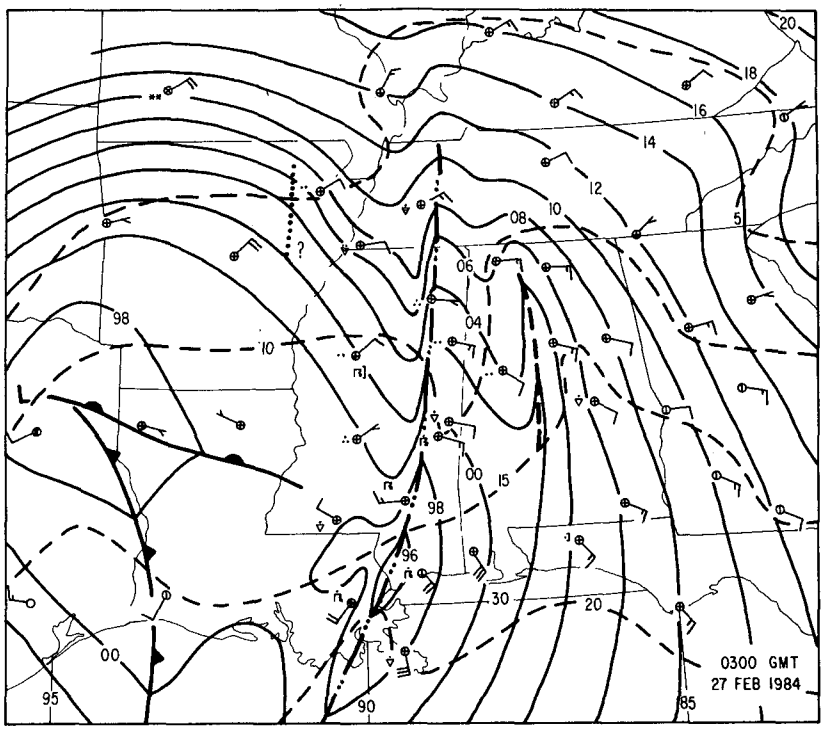

FIG. 12b. As in (a) except for 0300 UTC.

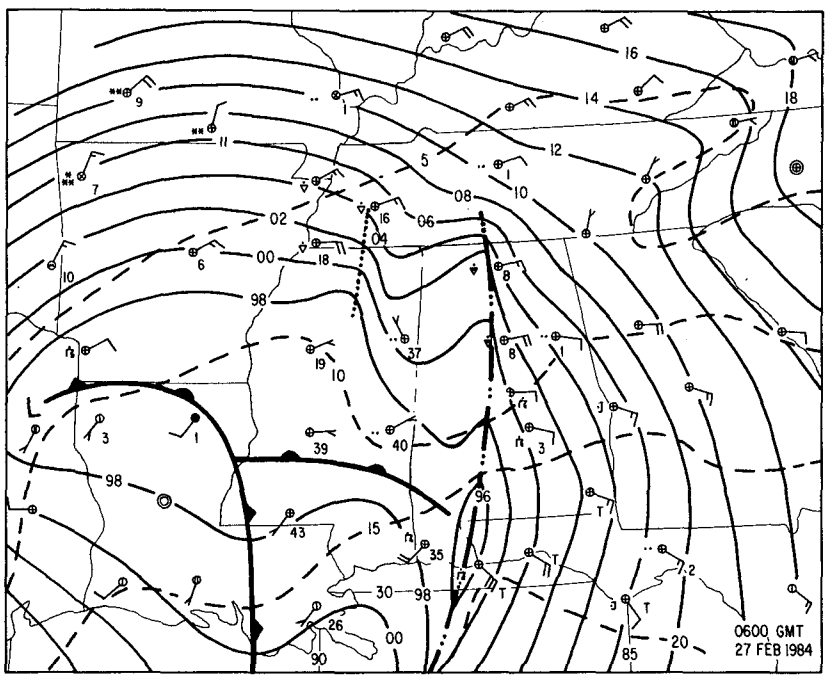

FIG. 12c. As in (a) except for 0600 UTC.

of the organizing gravity waves and through the baroclinic zone across Georgia. Thunderstorms continue in the prong of cool air represented by the skinny mesoscale north–south oriented pressure ridge from Asheville, North Carolina (AVL), southward through AHN. Comparison with the satellite-derived cloud top temperatures shown in Fig. 5, however, reveals that the thunderstorms occurring in the northern half of

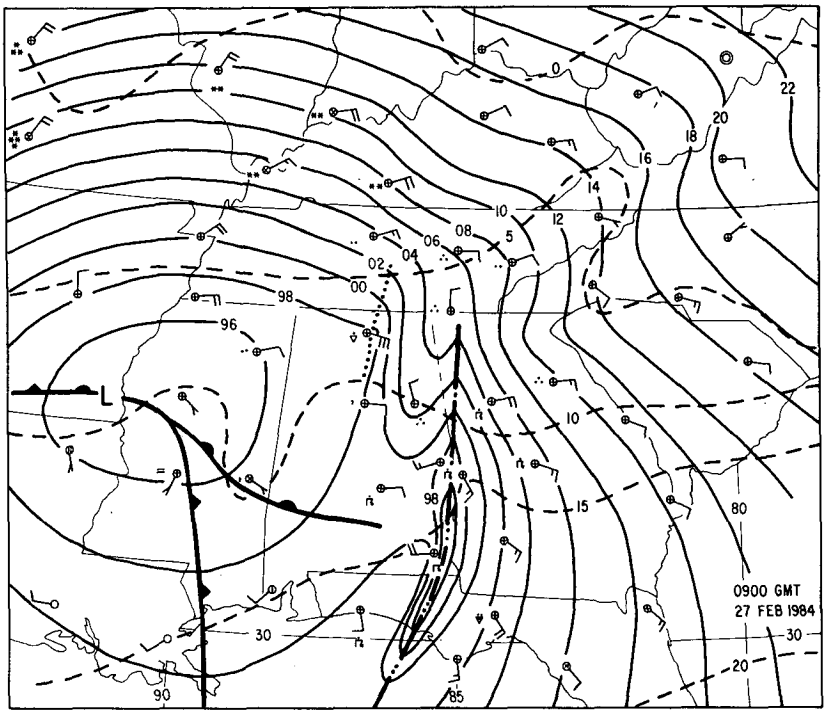

FIG. 12d. As in (a) except for 0900 UTC.

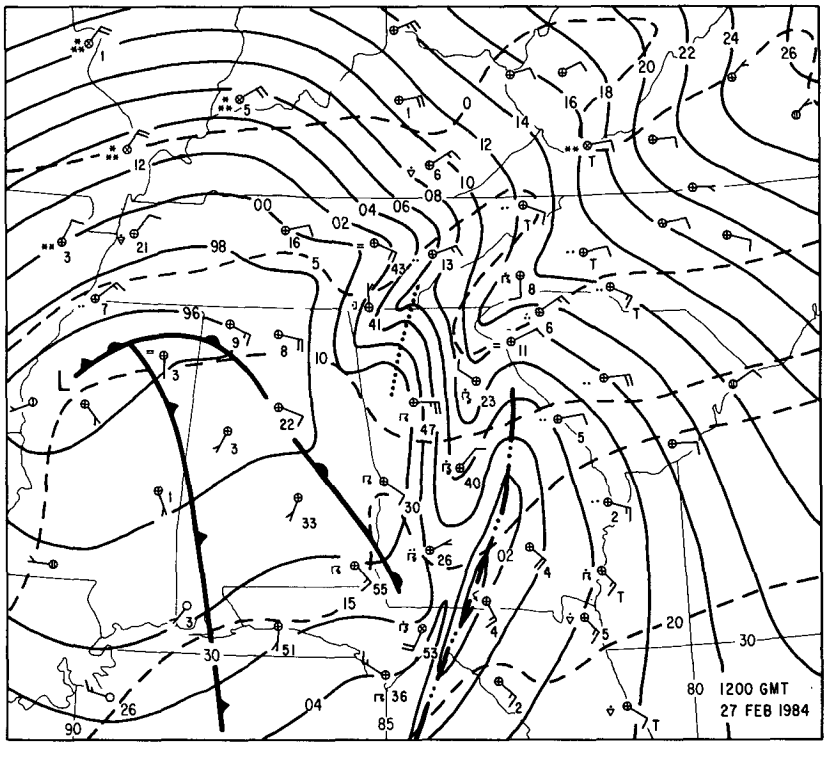

FIG. 12e. As in (a) except for 1200 UTC.

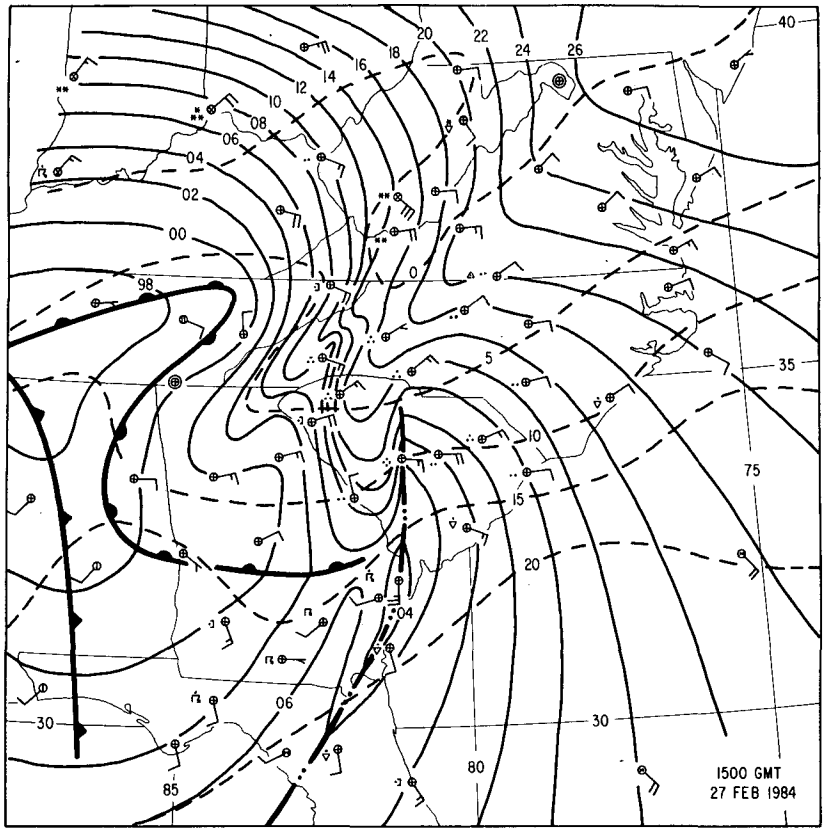

FIG. 12f. As in (a) except for 1500 UTC.

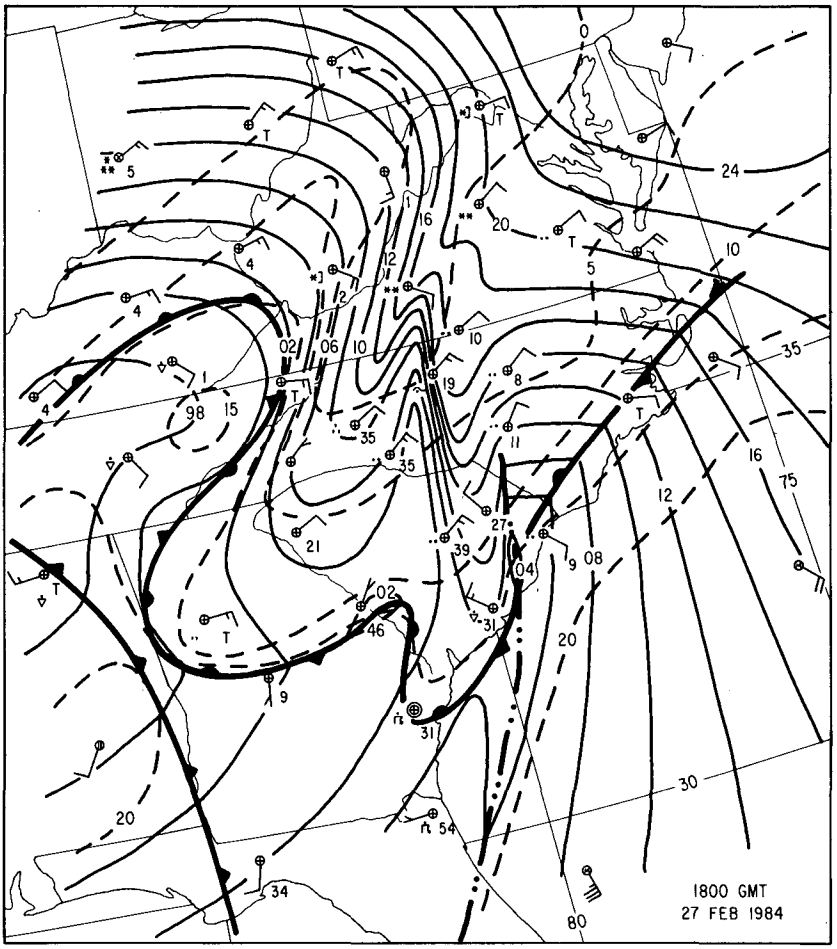

FIG. 12g. As in (a) except for 1800 UTC.

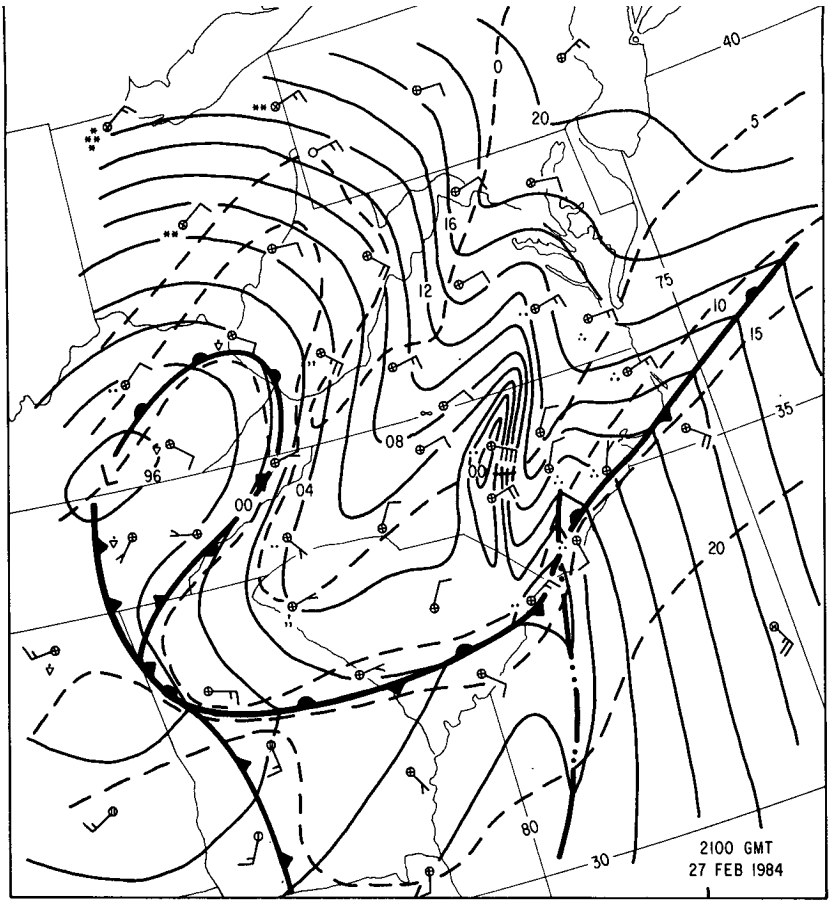

FIG. 12h. As in (a) except for 2100 UTC.

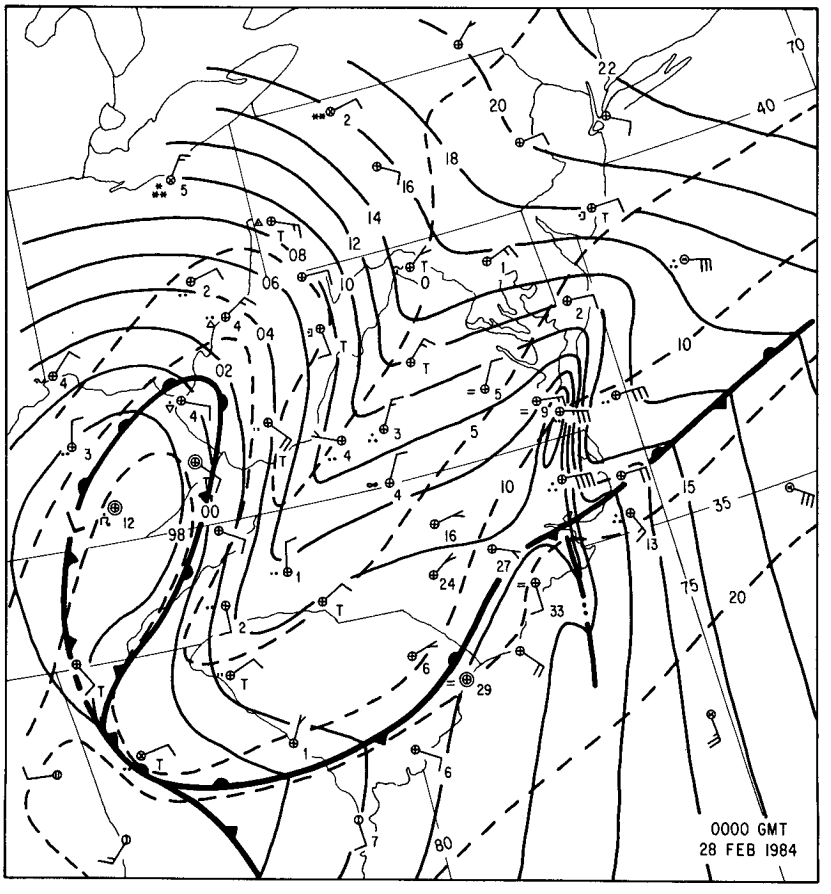

FIG. 12i. As in (a) except for 0000 UTC.

this pressure ridge are not associated with significantly cold cloud tops. Exceptionally heavy rains (30–55 mm) occur in conjunction with the convection, even well into the cold air. Behind the pressure ridge (e.g., ATL), the winds again become gusty from the east (peak speeds ~ 20 m s^{-1}) as pressures fall rapidly toward the sharpening wake trough and organizing gravity wave within the low-level cold air in extreme northwestern Georgia. The surface flow is divergent in this area of pressure falls, given the temporary westerly wind components (e.g., AHN) that occur in the narrow wedge ridge. The northern branch of the trailing pressure fall area in eastern Tennessee is along the western slopes of the highest mountains. Here, lee troughing is occurring under downslope easterly flow conditions, and over the next few hours numerous towns in the higher elevations of eastern Tennessee will report maximum wind gusts of 30–40 m s^{-1}. Within this region (recall Fig. 2 and to be more fully discussed in sections 5 and 7) there is evidence for the formation of a separate gravity wave after 1200 UTC.

The principal change by 1500 UTC (Fig. 12f) is the intensifying and narrowing wake trough from AHN northeastward past AVL. This trough now marks the locus of a well-defined pressure minimum associated with a rapidly strengthening gravity wave *east* of the Appalachian Mountains *within* the region of cold air damming and to the *west* of the decaying squall line from central South Carolina southward. Very strong (>30 m s^{-1}) surface wind gusts now extend into West Virginia [around Bluefield (BLF) and Beckley (BKW)] in response to the observed lee troughing west of the Appalachians (note the bulge of warm air into northeastern Tennessee) and a tightening of the cross mountain pressure gradient ahead of the advancing northern gravity wave, which appears as an enhanced pressure fall region on the barograms.

A very intense gravity wave lies to the west of a Danville, Virginia (DAN), to GSO line by 1800 UTC (Fig. 12g). It is moving eastward across the Piedmont region of the Carolinas at ~ 15 m s^{-1}. To the west of the mountains near Knoxville, Tennessee (TYS), the presence of a closed 15°C isotherm (the temperature reached 19°C there at 1700 UTC) is additional confirmatory evidence for the pocket of subsidence warming associated with the separate lee troughing in this region first mentioned in connection with the 1200 UTC map (Fig. 12e). The satellite cloud top temperature map closest to this time (1700 UTC, Fig. 5c) shows the gravity wave to be embedded in a region of relatively warm cloud tops between the squall line to the east and a patch of higher and colder clouds to the west. The troughing across the panhandles of West Virginia and Maryland into southwestern Pennsylvania is a manifestation of the advancing northern gravity wave. Precipitation is sparse with the northern wave (<1–2 mm) and continues heavy to the south.

By 2100 UTC (Fig. 12h) the main gravity wave is passing through the RDU region accompanied by sustained winds of 20 m s^{-1} (gusts in excess of 25 m s^{-1}), a dramatic pressure plunge of 14 mb and an abrupt cessation of precipitation (recall Fig. 1). The principal gravity wave is close to peak intensity, with the largest wave of depression amplitude found across central North Carolina to the Virginia border in the heart of the cold air damming region. The warm pocket west of the mountains has closed off, while the dissipating northern wave is barely detectable in New Jersey.

Finally, by 0000 UTC 28 February (Fig. 12i), the gravity wave is reaching the coast in the Norfolk, Virginia (ORF) area. The wave is now advancing at more than 15 m s^{-1} and will reach 20 m s^{-1} as it passes offshore during the next six hours. Left in the wake of the gravity wave is a bland weather map dominated by cold air damming east of the Appalachians with air blowing down the mean sea level pressure gradient at right angles to the isobars. A separate cyclonic circulation center remains to the west of the mountains in Kentucky along the western edge of the warm pocket. A coastal front is now firmly in place along the coast of the Carolinas, having been little disrupted by the passage of the decaying squall line.

5. Gravity wave characteristics

Station pressure time series for locations within the principal gravity wave formation area are displayed in Fig. 13. At LIT the squall line passes around 2000 UTC 26 February, accompanied by pressure perturbations of approximately ±1 mb. The wake high (+4–5 mb) follows by 2300 UTC with modest falls thereafter, including a small wavelike feature at 0000 UTC 27 February. Farther east at MEM the squall-line-induced pressure rise is more abrupt ($\sim$5 mb) just before 0200 UTC. The gradual fall thereafter is enhanced between 0400 and 0500 UTC as the aforementioned fall area (recall Fig. 12b) crosses the MEM area accompanied by minor pressure oscillations of +0.5 mb. (A more noticeable series of gravity waves is seen at MEM after 0700 UTC. These waves develop ahead of an area of modest convection in extreme eastern Arkansas and will not be discussed further as they have no bearing on our case.)

At Tupelo, Mississippi (TUP), and Huntsville, Alabama (HSV), a gravity wave signature in the form of an abrupt 3–4 mb pressure fall with little change thereafter is seen shortly after 0600 and 0800 UTC, respectively. The wave, which has time and space continuity with the enhanced falls at MEM ending at 0400 UTC, is amplifying in the *wake* of the squall-line-produced bubble high.

Across Tennessee at Chattanooga (CHA) and Knoxville (TYS) the wave structure is again more ambiguous. Time continuity places the wave at CHA around 1030 UTC and at TYS around 1200 UTC. Neither signal is clear cut, which suggests that the wave

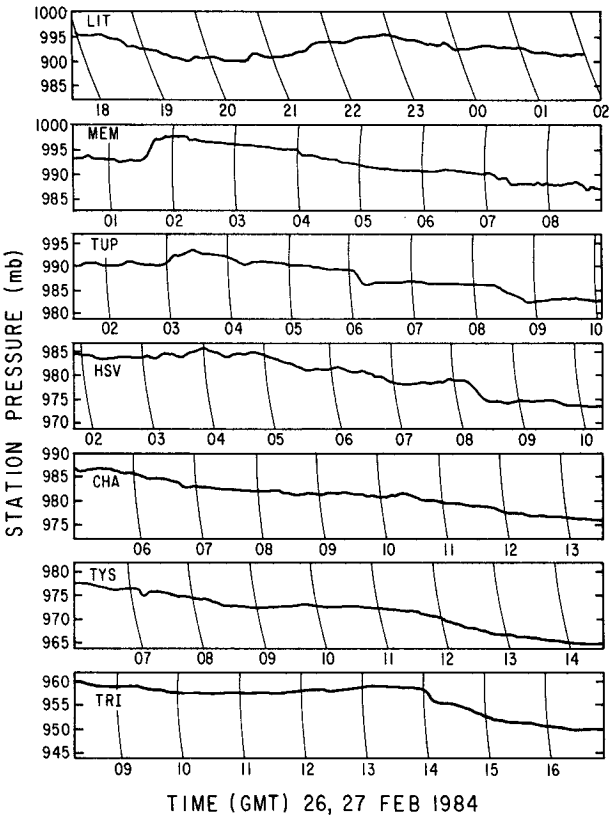

FIG. 13. 12 h station pressure time series barograms for Little Rock, Arkansas (LIT); Memphis, Tennessee (MEM); Tupelo, Mississippi (TUP); Huntsville, Alabama (HSV); Chattanooga, Tennessee (CHA); Knoxville, Tennessee (TYS); and Bristol, Tennessee (TRI) for 26–27 February 1987.

may have temporarily weakened or that the wave is more intense farther south in northwest Georgia where there are no observations. To the northeast at Bristol, Tennessee (TRI), there is evidence for wave regeneration in the mountains in the form of an abrupt 3 mb pressure plunge just after 1400 UTC. Also, at CHA, TYS and especially TRI there is evidence for the onset of larger scale pressure falls west of the Appalachians.

This point is reinforced in Fig. 14, which displays selected seven-day barograms for stations in Kentucky and Ohio eastward to the Atlantic coast. The enhanced falls at Bowling Green, Kentucky (BWG), around 0900 UTC match up with the HSV observations. Farther east in London, Kentucky (LOZ), the wave signature is more ambiguous, consistent with the picture at CHA and TYS. Across West Virginia [BLF, BKW, Elkins (EKN) and Martinsburg (MRB)], Pennsylvania [Altoona (AOO) and Harrisburg (CXY)] and south and eastward through Sterling, Virginia (IAD), Wilmington, Delaware (ILG), and Salisbury, Maryland (SBY), there is a characteristic signature of a rapid pressure plunge of ~4–7 mb in 1–2 h that begins around 1500 UTC in West Virginia and near 1800 UTC at ILG and SBY. This pressure fall region, even when allowing for the diurnal fall correction of 1–2 mb centered near 1800 UTC, is substantial. [For comparison see Zanesville, Ohio (ZZV) just to west of the swath of the pressure fall center.] While the signal differs among the various stations, the overall continuity is excellent and supports the interpretation of a gravity wavelike feature propagating rapidly northeastward (recall Fig. 2) at more than 30 m s^{-1}.

The northern portion of the more substantial southern gravity wave can be seen at BKW near 1530 UTC, more significantly at BLF near 1630 UTC (where southeasterly winds gusted to 30–35 m s^{-1}) and most impressively at Danville (DAN) and Norfolk, Virginia (ORF), east of the mountains at 2000 UTC and 0000 UTC, respectively. The southern gravity wave is characterized by a greater wave amplitude, a better defined wave of depression and an unmistakable tendency for the wave amplitude to increase rapidly from the mountains to the Piedmont.

There is some uncertainty in the preceding analysis as to the wave source region, wave propagation velocity and wave shape. An anonymous referee has stated that an objective cross-spectrum analysis of the type described by Stobie et al. (1983) would help to remove any ambiguity as to whether the wave originated near the Mississippi River or northwestern Georgia and whether there were two linear wave fronts or one highly nonlinear "bowed-back" wave. We are comfortable with our assertion that the primary wave originated near the Mississippi River and the secondary wave formed in northeastern Kentucky based upon our painstaking space–time continuity analysis blended together with meteorological information not available to a purely statistical objective analysis procedure.

Figure 15 shows a portion of the 12 h Atlanta, Georgia (ATL), barogram trace and tipping bucket precipitation record expressed as a 10 minute rainfall rate. Precipitation begins at 0700 UTC and slowly intensifies until the time of squall line passage at 1000 UTC,

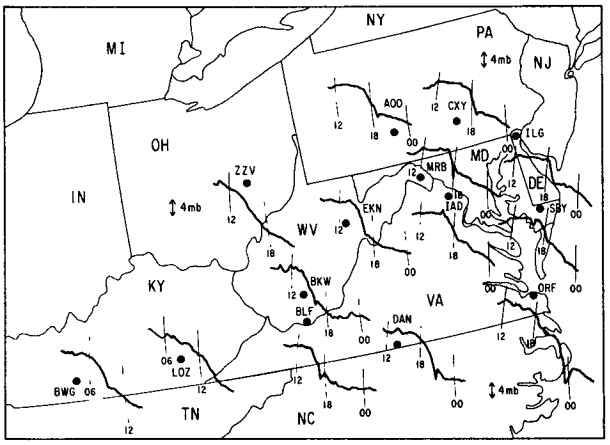

FIG. 14. As in Fig. 13 except for 7-day barograms for selected stations shown by solid circles.

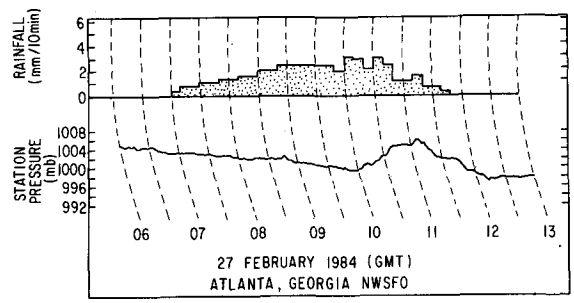

FIG. 15. Time section of accumulated 10 min precipitation (mm, top) and station pressure (mb, bottom) for Atlanta (ATL), Georgia, on 27 February 1984.

whereupon it becomes very heavy and showery (frequent thunder is observed throughout the period) with the 6–7 mb pressure rise ending at 1115 UTC. The rains continue and eventually taper off during the 8 mb pressure plunge in the hour period ending at 1215 UTC. The gravity wave is intensifying in this thunderstorm wake depression region, which extends northward across the Tennessee–North Carolina border.

At Greenville–Spartanburg, South Carolina (GSP, Fig. 16), nestled up against the eastern slopes of the Appalachians, the station pressure rises nearly 2 mb in the hour ending at 1500 UTC, followed by an impressive plunge of 7 mb in a few minutes (again, the horizontal gradient is drawn underestimated in Fig. 12f) and is then followed by pressure oscillations of ±1 mb for the next 2 h. Also shown in Fig. 16 is a trace of the accumulated precipitation, wind direction (eight point compass) and "miles" of air movement (the original trace is marked every time one mile of air moves past the instrument) converted to kilometers. Precipitation begins near 1100 UTC, falls hard until 1320 UTC, slackens somewhat until 1400 UTC and then pours down hard again before abruptly ending as the wave of depression arrives. Between 1400 and 1500 UTC the wind tends to lighten and become more north-northeast followed by a return to northeast and increase in speed with the pressure plunge (average velocity of ~ 17 m s^{-1} in the 1500–1530 UTC period versus 7 m s^{-1} over the previous hour). This interpretation is consistent with weak convergence during the brief wave of elevation and strong divergence during the pressure plunge.

The GSO barogram displayed in Fig. 17 reveals a transition to the trace seen at RDU (recall Fig. 1) in that there is a pressure recovery of 30%–40% following the steep plunge to the minimum pressure. The cessation of precipitation as the pressure begins to fall is consistent with the findings at GSP and elsewhere, as is the envelope of wind gusts retraced off the official recorder and lightly smoothed by hand to eliminate short period oscillations. As a crude measure of the horizontal divergence field, note that for a wave phase velocity of 15 m s^{-1} the average wind speed increases by ~ 5 m s^{-1} (winds out of the east) during the 30 minutes ending at 1930 UTC. This corresponds to $\partial u/\partial x \sim 2.0 \times 10^{-4}$ s^{-1} if we neglect north–south wind variations. A similar wind speed decrease of 8 m s^{-1} in the following 30 minutes yields a $\partial u/\partial x$ of $\sim -3.2 \times 10^{-4}$ s^{-1} for which similar caveats apply.

Observations of wind speed, wind direction, temperature, solar radiation, precipitation rate and station pressure recorded at North Carolina State University (NCSU) in Raleigh, North Carolina, (kindly furnished by Dave Barber and Jerry Watson) are displayed in Fig. 18. The peak wind gust of 29.1 m s^{-1} occurs near the pressure minimum and with the ending of precipitation. A temperature increase of 1°–2°C is observed in the hour ending at 2100 UTC as the pressure plunges and the rainfall slackens. A further increase of 2°–3°C occurs in the following hour after the rain ceases, the pressure rises and the winds decrease. Figure 18 shows that the observed warming that accompanies the passage of the gravity wave at NCSU and elsewhere (Fig. 19) is not a transitory feature typical of a propagating wave but instead marks the onset of a warmer temperature regime. Warming of 1°–4°C characterizes the passage of the pressure minimum at most locations within the cold air damming region. The warming is greatest along the eastern slopes of the Appalachians, where the wave is getting organized, and from interior eastern North Carolina into extreme southeastern Virginia, where the wave amplitudes are the largest. (There

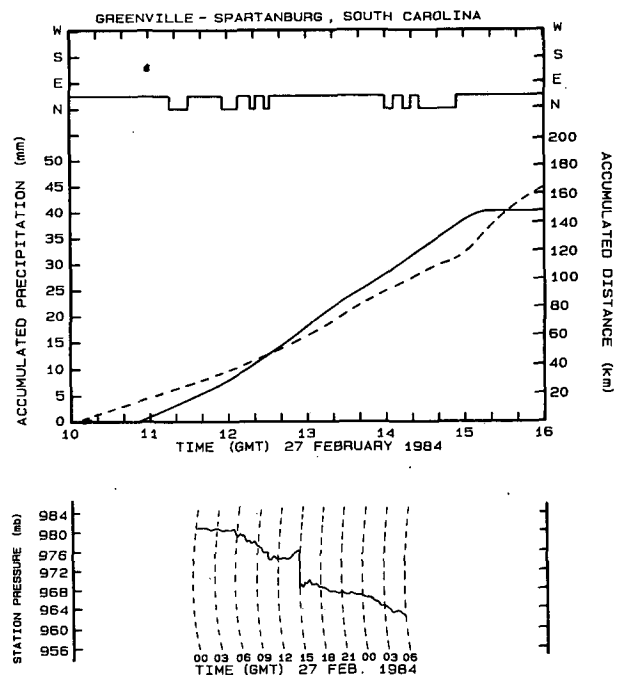

FIG. 16. (Top) Greenville–Spartanburg (GSP), South Carolina, time section of wind direction on an eight point compass; (middle) accumulated precipitation (solid, mm) and total air motion distance (dashed, km); and (bottom) station pressure (mb) for 27 February 1984. All times are UTC.

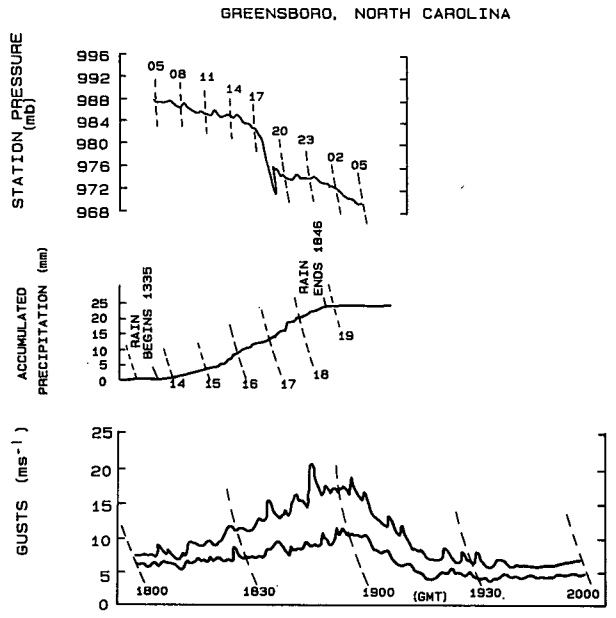

FIG. 17. Greensboro (GSO), North Carolina, time sections of (top) station pressure (mb); (middle) accumulated precipitation (mm); and (bottom) envelope of surface wind speed (m s^{-1}). All times are UTC.

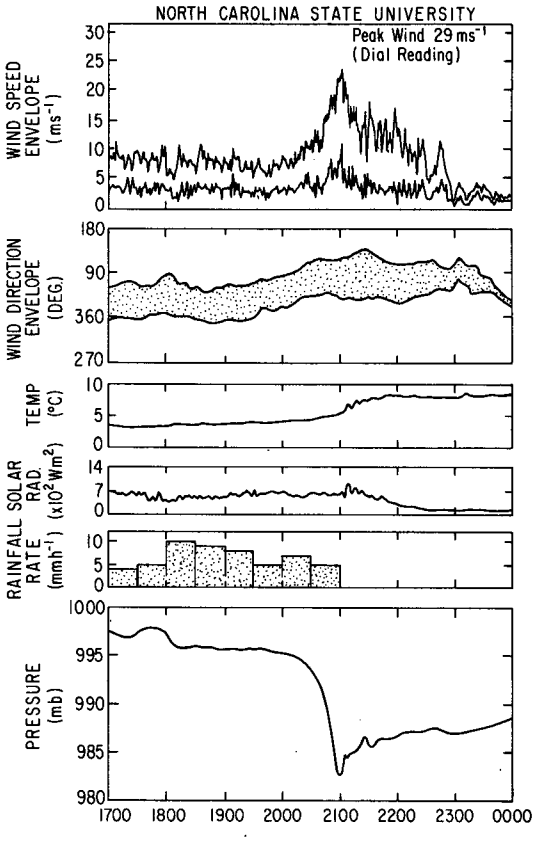

FIG. 18. North Carolina State University (NCSU) time sections of (a) wind speed envelope (m s^{-1}); (b) wind direction envelope (degrees); (c) temperature (°C); (d) solar radiation ($\times 10^2$ W m^2); (e) rainfall rate averaged for half-hourly periods (mm h^{-1}) and (f) station pressure (mb). All times are UTC.

is cooling along the immediate coast as the onshore flow regime is interrupted by the combined passage of the weakening squall line and trailing gravity wave.)

The origin of the warming is unclear. There is some evidence for a slight increase in solar radiation after 2100 UTC in Fig. 18, characteristic of wave-induced decreased cloud cover, but the approach of sunset renders this interpretation uncertain. A possible alternate interpretation is that the warming is triggered by wave-induced subsidence. To check this possibility, note that the surface pressure tendency can be expressed as

$$\frac{\partial p}{\partial t} = \frac{\rho c_p T_v w d\theta/dz}{\theta}. \quad (1)$$

On the basis of the GSO soundings shown in Fig. 11, we choose $d\theta/dz \sim 10°\text{C (km)}^{-1}$; $T_v \sim 280°$K, $\theta \sim 300°$K and $\rho \sim 1.0$ kg m^{-3}. Wave-induced subsidence of ~ 10 cm s^{-1} in the 1000–700 mb stable layer results in an estimated $\partial p/\partial t \sim 0.9$ Pa s^{-1} or ~ 9.0 mb $(17\text{ min})^{-1}$ in reasonable agreement with the observed tendency shown in Fig. 18. The physical mechanism involved is wave-induced mixing within the cold air dome. There are arguments against wave-induced subsidence warming, however. First, a narrow warm zone following the pressure minimum is not observed. Second, the 0000 UTC 28 February GSO sounding does not reveal explicit evidence for subsidence drying below 700 mb, although conditions may have changed since the passage of the wave 5 h earlier.

Again, some crude estimates of $\nabla \cdot \mathbf{V}$ can be made from the NCSU wind observations. Between 1830 and 1945 UTC (during heavy rain) the average gust speed is reduced 2 m s^{-1} while the wind veers 20°–25°. If we assume a wave phase speed of ~ 15 m s^{-1}, we obtain a value of $\partial u/\partial x \sim -4.0 \times 10^{-5}$ s^{-1} (where again $\partial v/\partial y$ has been ignored). Similarly, between 2000 and 2100 UTC (when the minimum pressure in the wave is reached and the rain ends) the wind increases ~ 10

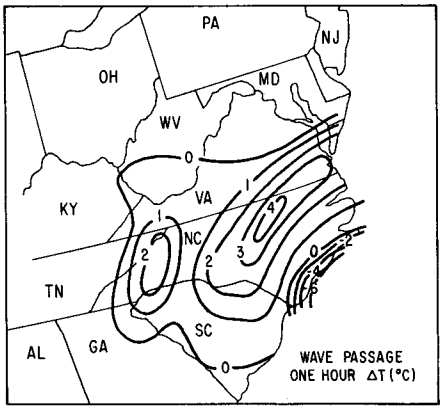

FIG. 19. One-hour temperature change (°C) accompanying passage of gravity wave on 27 February 1984.

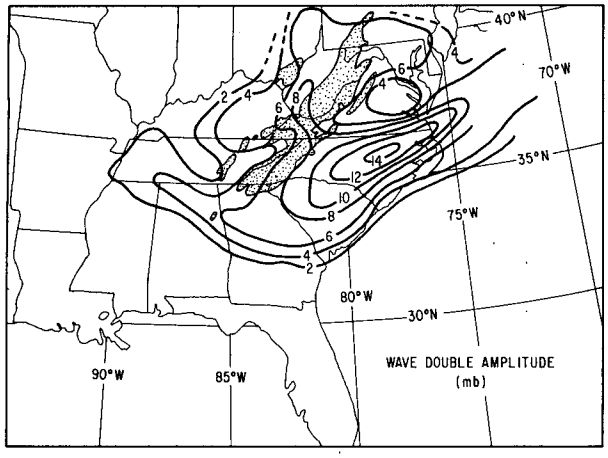

FIG. 20. Surface pressure decrease (mb) from wave crest to wave trough with passage of twin gravity waves on 27 February 1984. Stippling indicates terrain elevation > 600 m.

m s^{-1}, with a further veering to the east that yields an estimate of $\partial u/\partial x \sim 1.8 \times 10^{-4}$ s^{-1}. In the following hour, when the wind abates, a similar calculation yields an estimate for $\partial u/\partial x \sim -1.8 \times 10^{-4}$ s^{-1}. These wave-induced divergence values are comparable to those reported by Pecnick and Young (1984) for a similar large-amplitude gravity wave case in the Midwest.

Finally, Fig. 20 depicts the total pressure drop from wave of elevation crest to wave of depression trough (wave double amplitude). The amplitude of the principal southern gravity wave increases rapidly across the Appalachian Mountains, reaching a maximum in the cold air dome east of the mountains along a Charlotte, North Carolina (CLT)-RDU-ORF line. This line is oriented parallel to the mountains at the western end and lies parallel to, but 200–300 km north of, the coastal front boundary to the east. The analysis of wave amplitude is carried offshore with some uncertainty on the basis of hourly observations from several buoys. The northern wave amplifies across extreme eastern Kentucky and southwestern West Virginia and remains relatively unchanged eastward along the Pennsylvania–Maryland border before weakening rapidly over the immediate coastal plain.

A summary of the southern wave structure appears in a space–time diagram in Fig. 21 that takes advantage of the six surface stations located on a line nearly normal to the wave front in the Norfolk, Virginia area. Barograms were available from Newport News (PHF), Langley Air Force Base (LFI) and ORF. Noteworthy features of Fig. 21 include the following: 1) the veering and strengthening of the wind with the veering occurring first as the pressure begins to fall rapidly; 2) a reduction of precipitation intensity as the pressure falls abruptly; 3) a cessation of precipitation at the pressure minimum; 4) warming that begins in the rain area and continues after the pressure minimum is achieved and a southeasterly flow off the ocean is established and 5) a wave phase velocity of 60 km h^{-1} (~17 m s^{-1}) with the largest pressure perturbation to the southeast at the Norfolk Naval Air Station (NGU), ORF and Oceana (NTU). The maximum reported wind gusts from land stations in the Norfolk area were ~25 m s^{-1}. However, sustained winds at this speed were observed over water at the South Island pier of the Chesapeake Bay Bridge-Tunnel linking Norfolk with the Delmarva peninsula.

6. Radar-derived precipitation structure

Precipitation intensity maps, as derived from operational National Weather Service radar logs and supplemented by 16 mm radar film loops, are presented in Fig. 22. The contoured intensity levels correspond to the operational VIP level convention. At 0235 UTC 27 February (Fig. 22a) a squall line with patchy VIP level 3 and 4 intensity echoes runs from western Tennessee to southeastern Louisiana. The squall line is embedded within a large area of stratiform precipitation. The highest cloud tops are found to the south (13.1 and 13.4 km), where the squall line is active along the Louisiana–Mississippi border. In southwestern

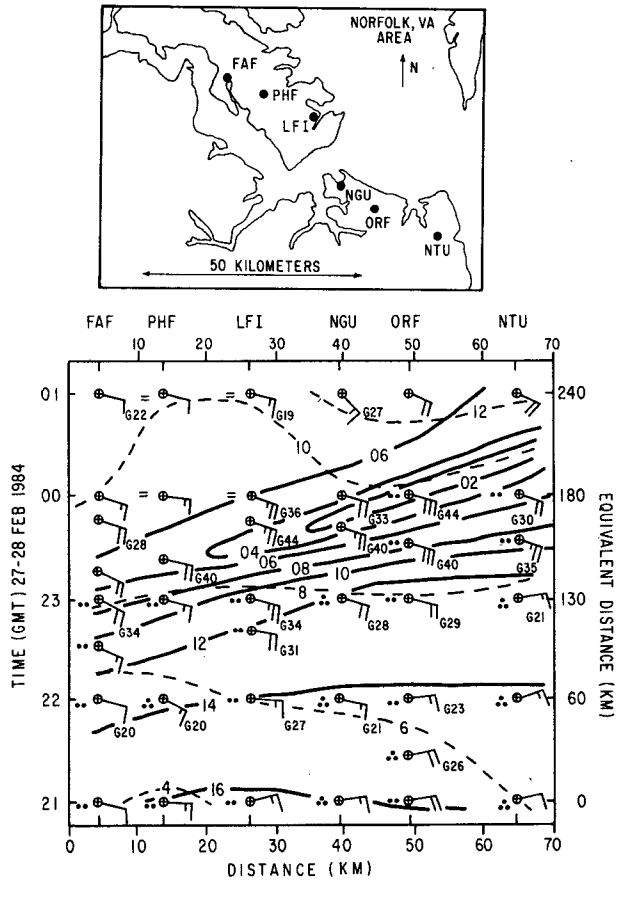

FIG. 21. Time series of winds (m s^{-1}), altimeter setting (solid, mb) and temperature (dashed, °C) for primary gravity wave passage in the Norfolk, Virginia, area. Station locations shown by insert at top. Data plotting according to Figs. 2 and 3.

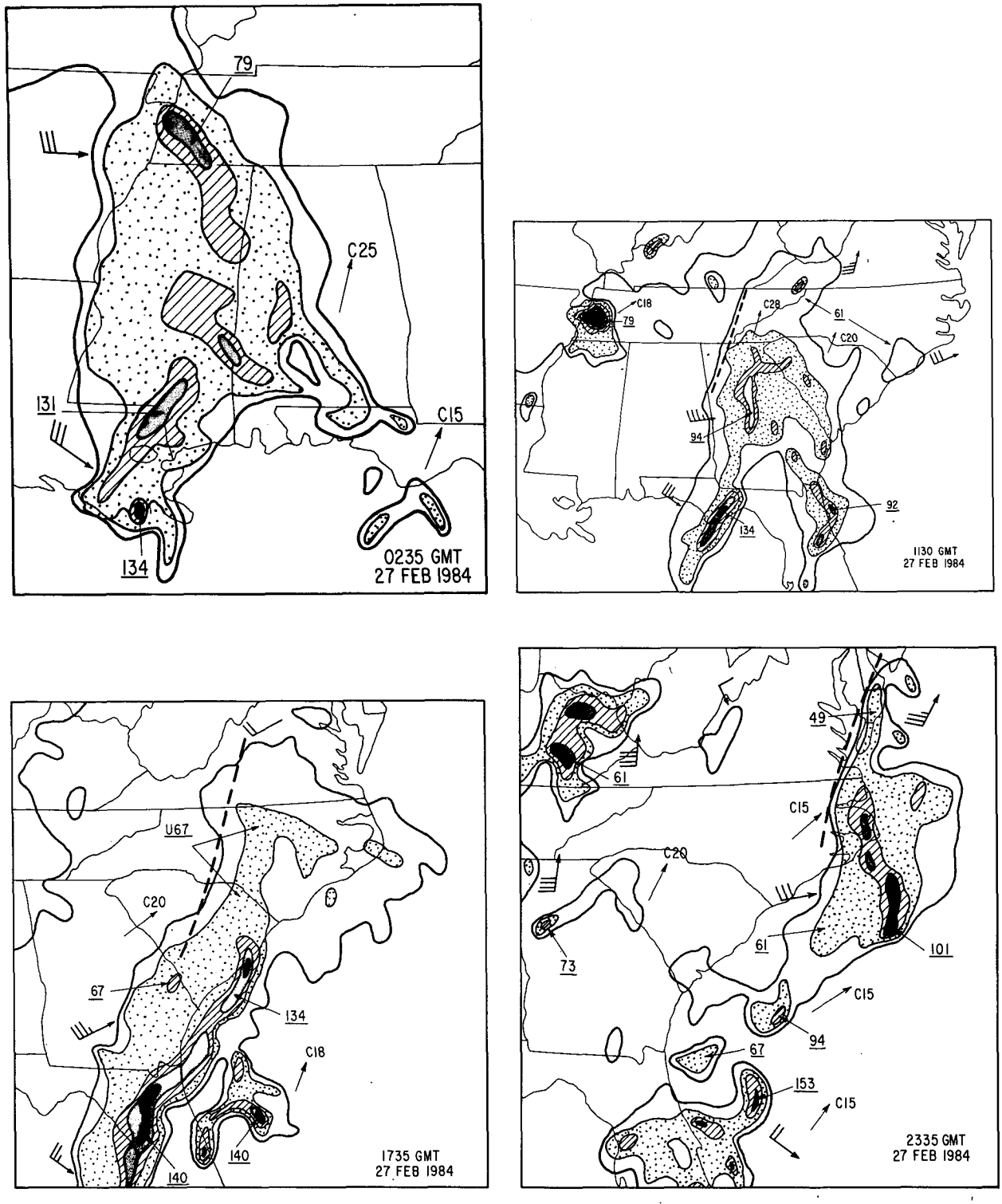

FIG. 22. National Weather Service manually digitized radar intensity (VIP) maps for (a) 0235, (b) 1130, (c) 1735, and (d) 2335 UTC 27 February 1984. Intensity levels as follows: VIP 2 (dotted), VIP 3 (hatched), VIP 4 (stippled) and VIP 5 (solid). Cloud top heights ($\times 10^2$ m) are underlined. Cell movement (C) in m s^{-1}; Uniform cloud tops indicated by prefix U. VIP levels 2–5 correspond to dBZ ranges of 30–41, 41–46, 46–50 and 50–57 respectively for the NWS WSR57 10-cm radars.

Tennessee equally intense precipitation echoes are associated with clouds topping out at 7.9 km. Significantly, the incipient gravity wave activity in the MEM area between 0300 and 0400 UTC (Fig. 13) is found *upstream* of a band of moderate convection.

By 1135 UTC (Fig. 22b) the southern half of the squall line has weakened slightly (level 4 echoes, maximum tops down to 13.4 km), while the northern portion across Georgia has intensified (level 4 echoes, maximum tops to 9.4 km). The area in northwestern Georgia and adjacent Tennessee and North Carolina where the gravity wave is now rapidly organizing lies along the northwestern edge of the main precipitation shield. A general cessation of precipitation occurs in the wake of the gravity wave over the next 6 h (Fig. 22c). The gravity wave, after initial intensification in the *wake* of active convective elements, continues to strengthen and move away from the mountains despite a considerable decrease in the intensity of the original convection. As the intense wave approaches the coast, it continues to lie along the trailing edge of the main precipitation shield. At 2335 UTC (Fig. 22d) the gravity wave signature in the radar echoes from ORF to WAL is particularly well defined. A narrow band of VIP level 2 cells is crossing the southern portion of the Delmarva peninsula. Maximum tops are down to 4.9 km, but the passage of this line of echoes is immediately followed by a surface pressure plunge of 10–12 mb in <30 minutes with gusty easterly winds over 25 m s^{-1}.

7. Discussion

a. Wave genesis mechanisms

Uccellini and Koch (1987), in a study of 13 cases of mesoscale wave disturbances of amplitude several millibars, period 1–4 h and horizontal wavelength 50–500 km, were able to isolate a synoptic-scale signal common to the majority of cases. In most cases the wave activity developed north of a surface frontal boundary in the presence of a prominent thermal inversion in the lower troposphere. The flow aloft was southwesterly, and there was a jet streak propagating toward a downstream ridge axis. In general, the surface location of the wave activity was sandwiched between the jet streak to the west, a ridge axis to the northeast, a frontal boundary to the south or southeast and an inflection point in the geopotential field aloft immediately to the southwest. They suggested that mesoscale gravity waves can, in general, be explained as part of a geostrophic adjustment process. Some doubt was cast upon shearing instability as a dominant wave genesis mechanism since a critical level was not found in all cases.

The possible cause and effect relationship between gravity waves and convection remains obscure. As noted by Uccellini and Koch (1987) there are published cases of large amplitude gravity waves in the literature (e.g., Pecnick and Young 1984) in which there is no apparent relationship between deep convection and wave amplitude. Lin and Goff (1987) provided some evidence for deep convection as a source region for a gravity wave that rapidly propagated away from the convective area. It is also of interest that they found that the wave formed on the north side of the convection, similar to the present case. Bosart and Sanders (1986) documented a case in which disorganized wave activity developed in the presence of modest midtropospheric convection and beneath a shear layer in advance of a propagating jet streak. The gravity wave, which during its intense phase was marked by exceptionally heavy snowfall rates and thunder and lightning, became especially well organized in an environment of strong frontogenetical forcing. Geostrophic adjustment processes could not be ruled out, however, because the wave environment was consistent with that described by Uccellini and Koch (1987).

The LIT sounding for 0000 UTC 27 February, shown in Fig. 23, is representative of environmental conditions near the suspected wave genesis region. The lower troposphere below 700 mb at LIT is very stable north of the surface frontal boundary and is in very good agreement with conditions found 12 h later (recall Figs. 7 and 9). Aloft, the atmosphere over LIT is saturated through a deep layer. There is little vertical wind shear below 500 mb, in marked contrast to the large shears observed at CKL, AHN and BNA at 1200 UTC 27 February.

Moreover, the thermal wind in the 700–200 mb layer is from the south-southwest, an orientation nearly parallel to the incipient wavelets shown in Fig. 2. This observation reduces the likelihood that shearing instability is an important wave genesis mechanism, as a critical level cannot be achieved. The strongest wind in the LIT sounding is 46 m s^{-1} at 385 mb, and the maximum shear is ~15 m s^{-1} over the 6.5 to 7.5 km layer. Given a 4°C potential temperature increase through this layer, a Richardson number of ~0.5 is computed. Nowhere in the sounding does the Richardson number fall to 0.25, further reducing the likelihood that shearing instability is an important wave genesis mechanism for the southern gravity wave.

Figure 24a shows the vertical profile of inverse Richardson number $(Ri)^{-1}$ and Brunt–Väisälä frequency (N) for 1200 UTC 27 February soundings at AHN, CKL and BNA (actual soundings appear in Figs. 8 and 9). Soundings using all available standard and significant level temperature and wind observations were plotted and then centered differences were employed over 50 mb thick layers to derive the preceding computations. The corresponding vertical profiles of wind speed relative to the phase velocity of the southern wave (17.0 m s^{-1} directed toward 100°) are presented in Fig. 24b. At BNA, to the northwest of where the wave intensifies, there is a shallow critical layer near 300 mb where the wave phase velocity matches the background wind in the direction of wave propagation. Simulta-

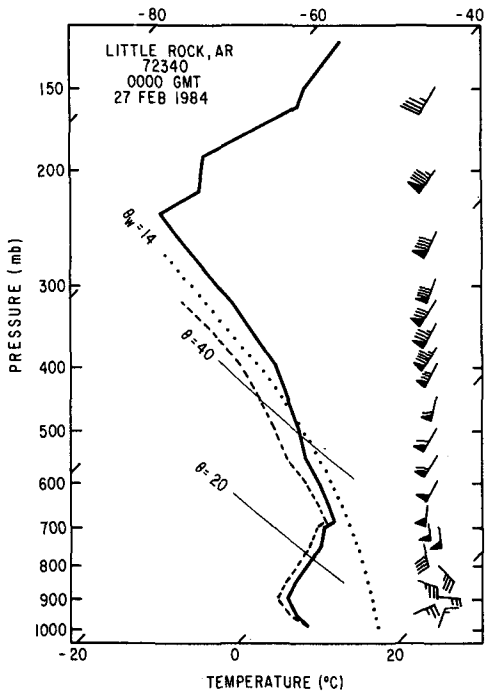

FIG. 23. As in Fig. 8 except for Little Rock, Arkansas, at 0000 UTC 27 February 1984.

neously, the value of $(Ri)^{-1}$ approaches 4 (or Ri $\sim$ 0.25), which suggests the possibility of shearing instability as a wave source in the upper troposphere. (One note of caution: the 50 mb thick averaging layer is likely to smear out shear and stable layers and thus reduce N and increase Ri from their true values.) A much lower critical layer is seen at CKL (730 mb) and AHN (625 mb) along the southern boundary of the wave amplification region. The critical layer at 730 mb at CKL reflects the exceptionally strong shear, culminating in a wind in excess of 50 m s^{-1} at 600 mb, seen at that location in Fig. 9. The Richardson number lies between 0.50 and 0.25 in much of the 850–600 mb layer at CKL, while N is relatively small in most of this layer, with higher values above and below. At AHN the Richardson number is <1 near the critical layer at 625 mb. The strong wind shear in the 800–600 mb layer at CKL originates at the eastern end of a subsiding midtropospheric frontal zone, while the lower tropospheric shear layer at AHN is more of a reflection of the aforementioned low-level jet.

The orientation of the northern gravity wave from northwest to southeast (recall Fig. 2) is nearly normal to the thermal wind at the immediate upstream sounding stations of AHN, CKL and BNA (Figs. 8 and 9). With an observed wave phase velocity of $\sim$30 m s^{-1}, a critical layer near 700 mb (refer to Figs. 8 and 9) is indicated at all three stations. Moreover, Fig. 24a indicates that just below 700 mb the Richardson number is <0.25 at BNA and close to 0.25 at CKL. A similar

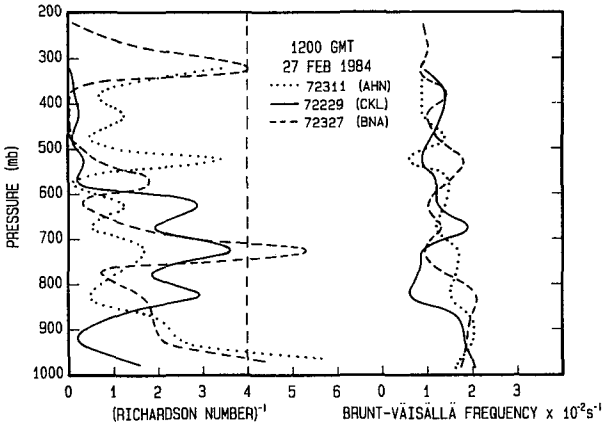

FIG. 24a. Plots of inverse Richardson number and Brunt–Väisälä frequency ($\times 10^{-2}$ s^{-1}) versus pressure (mb) for Nashville, Tennessee (BNA); Centreville, Alabama (CKL); and Athens, Georgia (AHN) for 1200 UTC 27 February 1984.

critical layer is found at LIT 12 h earlier (Fig. 23) near 450 mb at the base of the 1 km layer over which the Richardson number is 0.5. Hence the available evidence suggests that environmental conditions over the Tennessee Valley at 1200 UTC 27 February upstream of the area in which the northern gravity wave originated are favorable for wave generation by shearing instability.

A second possible wave genesis mechanism is geostrophic adjustment. For a disturbance of scale small compared to the Rossby radius of deformation (e.g., a propagating jet streak), the mass field tends to adjust to perturbations in the wind field. Using a linear theory for a stratified atmosphere, Blumen (1972) was able to show that the Rossby radius of deformation wavelength could be written as

$$L_R \sim \frac{NH}{2\pi f} \tag{2}$$

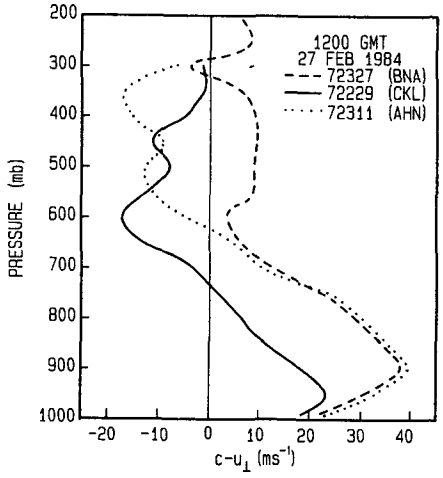

FIG. 24b. As in Fig. 24a except for gravity wave phase velocity relative to normal wind component (m s^{-1}).

where H is the atmospheric scale height. For typical values of N ($\sim 1.2 \times 10^{-2}$ s^{-1} from Fig. 26a) and $H \sim 10$ km, we compute an $L_R \sim 230$ km at 35°N. In effect, L_R represents the gravity–inertia wavelength. With an observed wavelength of 100–150 km in the present case, we see that gravity inertia waves are possible although the energy source remains unknown. Van Tuyl and Young (1982) examined the geostrophic adjustment process when alongstream flow variations were allowed. They found that gravity–inertia waves could be excited just downstream of high velocity jet cores in a region of strongly increasing divergence and large Rossby number. Typically, such a flow configuration would be found in the diffluent exit region of a propagating jet streak approaching a downstream ridge as exists in the present case.

Figures 25a, c depict the 200 and 300 mb divergence computed on a one degree latitude–longitude grid mesh for 1200 UTC 27 February. Superimposed on the divergence field are selected isotachs and ageostrophic wind vectors (vector difference between the observed and geostrophic wind). At 200 mb an axis of maximum divergence ($>10 \times 10^{-5}$ s^{-1}) lies above the squall line from southern Georgia into the Gulf of Mexico with a secondary maximum lobe in the vicinity of the Georgia, North Carolina and Tennessee borders. In this latter region the ageostrophic wind vector rotates anticyclonically toward lower heights, with an implied acceleration to the northeast and east in the right entrance region of the 70 m s^{-1} 200 mb jet streak.

The 300 mb divergence at 1200 UTC is a maximum in an arc from east-central Tennessee southward across western Georgia and then southwestward in the Gulf of Mexico. Maximum divergence values exceed 8 $\times 10^{-5}$ s^{-1} in the band that overlies the southern gravity-wave intensification area and is located to the east of the 300 mb jet streak. The ageostrophic flow at 300 mb across eastern Tennessee, northern Georgia, eastern Kentucky, Virginia and the Carolinas is weakly from the west-southwest, a direction again consistent with quasi- and semigeostrophic theory expectations.

As an additional check on the possibility of geostrophic adjustment as a mechanism for gravity wave genesis, the ratio of the absolute value of the horizontal divergence to the absolute vorticity (an approximate measure of the ratio of the divergent to rotational flow) is displayed in Figs. 26a, b for 200 and 300 mb at 1200 UTC 27 February. This ratio approaches and exceeds unity from the northern Gulf of Mexico, northward across Georgia and the Tennessee and Ohio Valleys to the lower Great Lakes along the jet stream corridor. These calculations establish that geostrophic adjustment must be considered as an important physical mechanism in the rapid amplification of the principal southern gravity wave after 1200 UTC as it began to cross the Appalachian Mountains. Similarly, the possibility that geostrophic adjustment acts as an important companion to shearing instability in the generation of the northern gravity wave cannot be ruled out.

Evidence has already been presented that the southern gravity wave probably was triggered in western Tennessee and northern Mississippi after 0300 UTC 27 February. The position of the 300 mb ridge line, 300 mb jet, 850 mb low-level jet and surface frontal boundary (recall Figs. 3 and 4) at 0000 UTC 27 February with respect to the gravity wave source region is in keeping with the model of Uccellini and Koch (1987) in which geostrophic adjustment plays an important role in wave organization and maintenance. We have not carried out a similar set of calculations as in Figs. 25 and 26 for this time to test this assertion. Rather, we have chosen to concentrate on understanding why the amplitude of the southern gravity wave became so large.

The preceding analyses showed that the spatial relationship between the trailing gravity wave and leading squall line was maintained throughout the lifetime of the wave. The northern end of the squall line in Georgia was most intense around 1200 UTC 27 February at which time the southern gravity wave was beginning to amplify rapidly. Subsequently, the wave remained strong and persistent even though the convection slowly weakened. These observations indicate that convection may be playing some role in the organization and intensification of the southern gravity wave. Branick et al. (1988), in a study of a long-lived mesoscale convective system, also presented evidence for the development of a large amplitude pressure oscillation in a trailing wake depression behind the convective complex.

One possible physical mechanism is a wake depression (using terminology originally defined by Fujita 1959) to the rear of the squall line. Hoxit et al. (1976), in a discussion of mesolows or pressure troughs in advance of cumulonimbus clouds, also alluded to the possibility of a similar trough in the wake of a convective system. Figure 27 shows the location and time of all reported thunderstorms tabulated from the dense surface observing network on 27 February 1984. In general, most of the thunderstorms are associated with the passage of the principal squall line. Exceptions include a batch of thunderstorms in extreme western Tennessee and Kentucky into southern Illinois near 1200 UTC and over extreme eastern Tennessee and western North Carolina at about the same time. These latter thunderstorms are modest and devoid of high cold cloud tops (recall Fig. 5). There are also scattered, but modest, thunderstorms in the vicinity of the organizing wave itself. The radar maps in Fig. 22 clearly show that the gravity wave forms in the wake of a line of VIP 3 (some embedded VIP 4's) intensity cells. The cross sections (Fig. 6), 850 mb sectional map (Fig. 4) and soundings (Figs. 8, 9) all reveal that warm, moist unstable air is advected rapidly northward by a strong

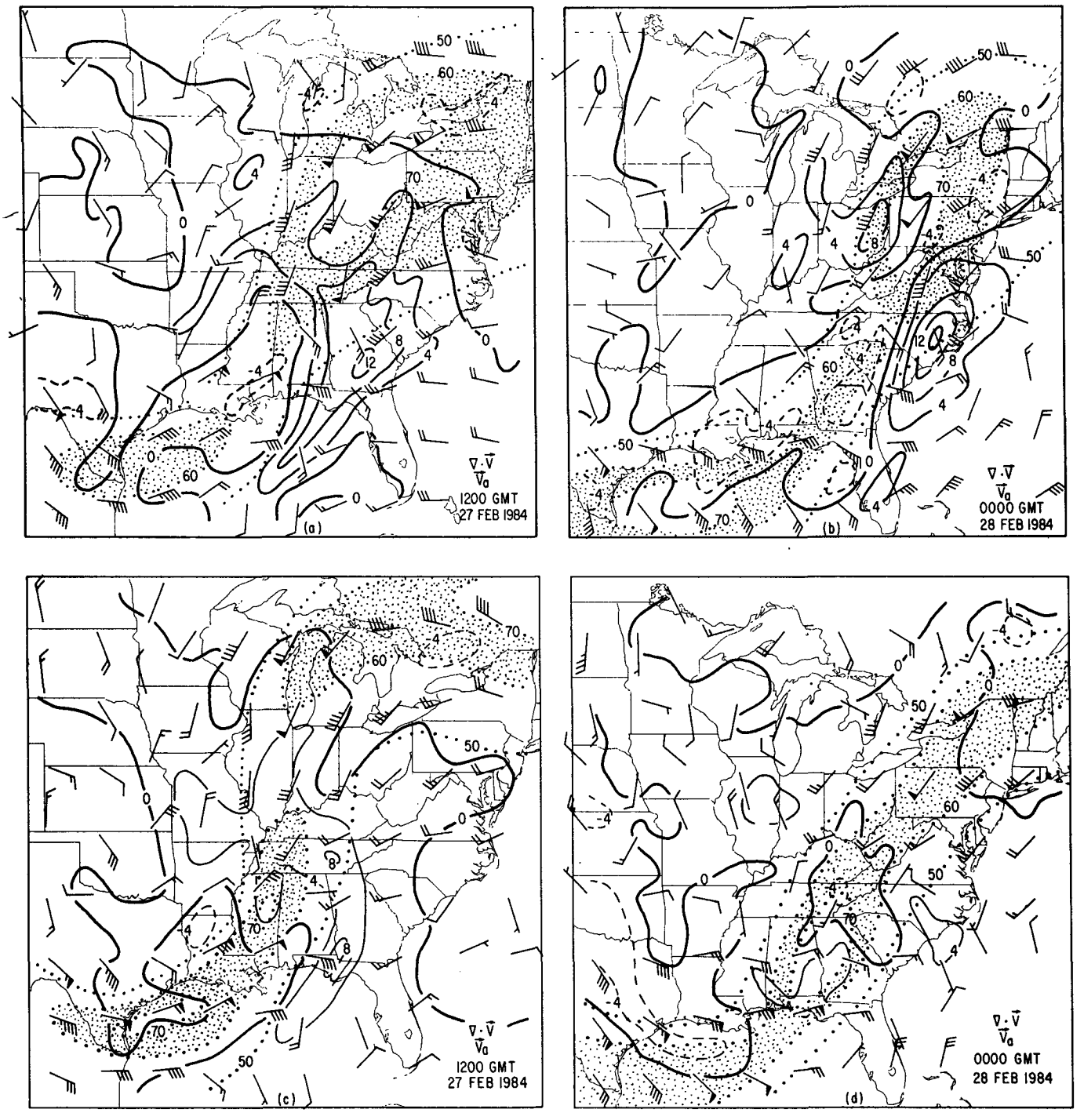

FIG. 25. Divergence ($\times 10^{-5}$ s^{-1}) with superposed ageostrophic wind components (m s^{-1}; displayed every 3° latitude-longitude) and 50, 60 and 70 m s^{-1} isotachs (60–70 m s^{-1} band stippled). Divergence (convergence) contours are solid (dashed) with zero isopleth heavy solid: for 200 mb at (a) 1200 UTC 27 February and (b) 0000 UTC 28 February 1984; (c) and (d) as in (a) and (b) except for 300 mb.

low-level jet above relatively cold and stable boundary layer air. Thunderstorms erupt in the overriding plume of warm, moist unstable air in response to favorable synoptic scale forcing.

At 1200 UTC 27 February there is a deep layer of vigorous ascent running along and just ahead of the low-level jet (peak values of -18×10^{-3} mb s^{-1} in the 700–500 mb layer as computed kinematically but not

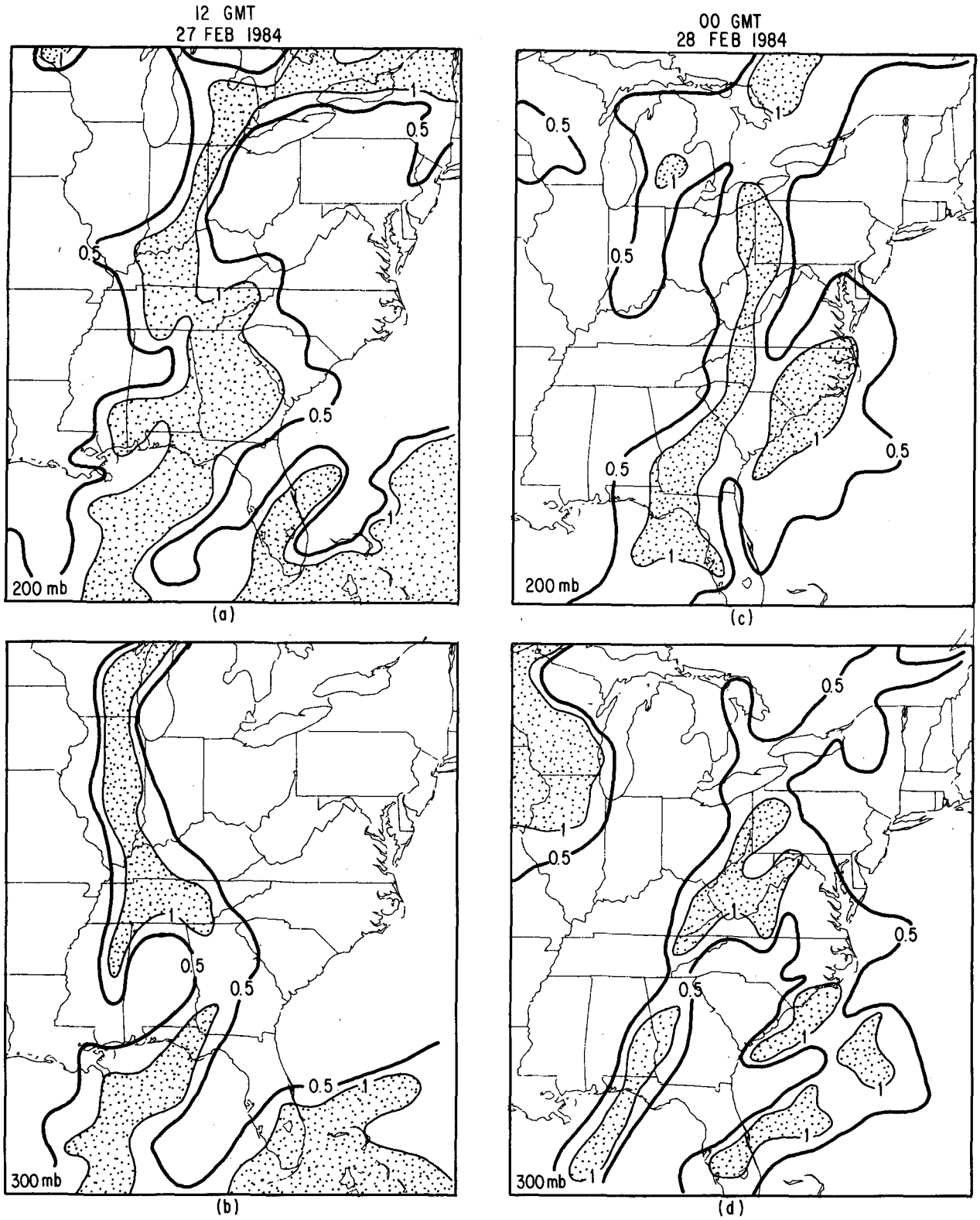

FIG. 26. Ratio of the absolute value of the horizontal divergence to the relative vorticity for (a) 200 mb 1200 UTC 27 February 1984; (b) 300 mb 1200 UTC 27 February 1984; (c) 200 mb 0000 UTC 28 February 1984; and (d) 300 mb 0000 UTC 28 February 1984. Ratios contoured for 0.5 and 1.0 with values ≥ 1.0 stippled.

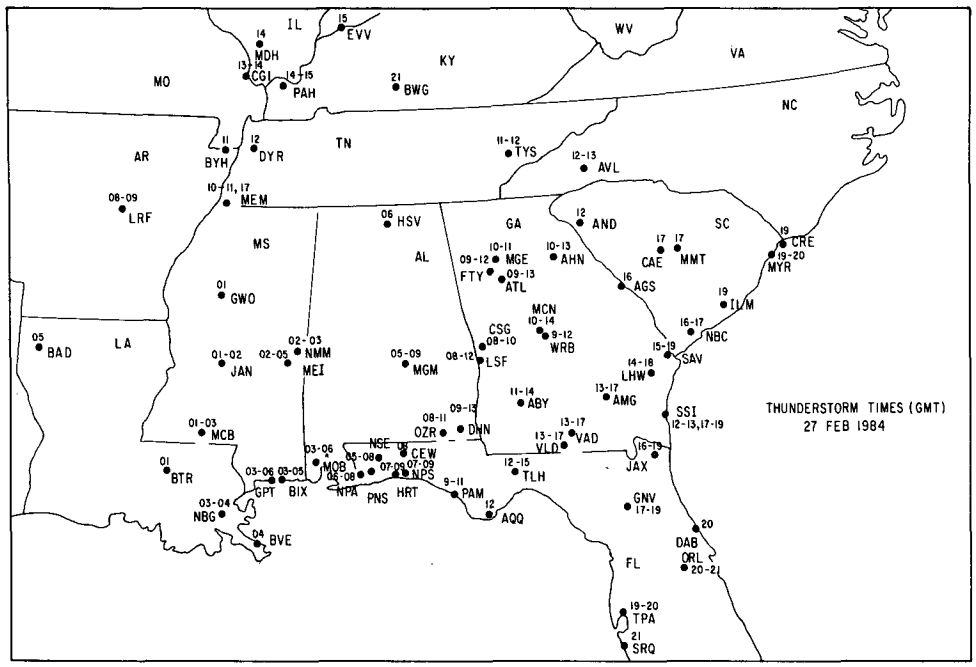

FIG. 27. Instances of thunder as reported by the surface network on 27 February 1984. Times (UTC) rounded to the nearest hour.

shown here) associated with the thunderstorms. The ascent region tilts gradually westward with height from northern Florida northward across Georgia into eastern Tennessee and western Kentucky. It may be possible that vigorous compensating subsidence behind the line of convection into the entrenched cold, stable boundary-layer air acts to help organize and intensify the gravity wave. This is analogous to the genesis mechanism discussed by Lin and Goff (1987) with diabatic heating replaced by adiabatic compression as a source mechanism for the solitary wave.

There are at least two major problems with the wake low hypothesis. First, it is necessary to explain why the wake low is not triggered farther south where the squall line is more vigorous. Second, an explanation is required of how subsidence can trigger such a large amplitude and persistent gravity wave. An earlier calculation in section 5 showed that subsidence of ~ 10 cm s^{-1} could produce a surface pressure fall of ~ 9 mb $(20\ \text{min})^{-1}$, given the observed stratification across the Carolinas. From Fig. 7a it is seen that the stability below 700 mb at 1200 UTC 27 February increases eastward from the Mississippi River Valley and is most intense east of BNA across the Appalachian Mountains. Farther south over northern Florida, the boundary layer is much less stable, as shown, for example, by the AQQ sounding in Fig. 8. Consequently, the potential for adiabatic warming and a lowering of surface pressure due to subsidence is considerably reduced where the convective elements in the squall line have their roots in the boundary layer. To the north within the region of cold boundary layer air, it is at least possible that a trailing wake low behind the squall line can be enhanced by a thermally direct circulation across the line. What is not explained is the abrupt intensification of the gravity wave as it crossed the mountains.

b. *Wave maintenance*

Lindzen and Tung (1976) were able to show that gravity waves of appreciable amplitude and phase speeds of order a few tens of meters per second could propagate without appreciable decay through a prominent stable layer (duct) provided the duct lay below a much deeper layer of marginal stability that contained a critical layer in the presence of Richardson number ~ 0.25. This configuration allowed appreciable wave reflection and enabled the wave to propagate over a long distance with little loss of energy. Figure 28 shows the vertical profiles of N, $(\text{Ri})^{-1}$ and $(c - u_\perp)$ for WAL at 0000 UTC 28 February in the same format as Fig. 26. Recall that the WAL sounding (Fig. 10) was taken at the time the wave of depression was traversing the station. There is a deep critical layer above 550 mb, although the Richardson number is not particularly small, because of the lack of appreciable vertical wind shear. The N profile, however, is favorable for sustained wave ducting.

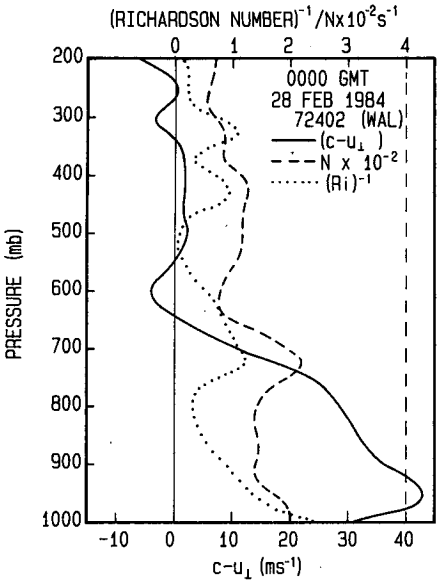

FIG. 28. Gravity wave phase velocity relative to normal wind component (m s^{-1}, bottom) and inverse Richardson number and Brunt–Väisälä frequency ($N \times 10^{-2}$ s^{-1}, top) versus pressure (mb) for Wallops Island, Virginia (WAL) at 0000 UTC 28 February 1984.

If we take the expression used by Bosart and Sanders (1986) to test the Lindzen and Tung (1976) ducted gravity wave model,

$$c_{\text{duct}} = \frac{1}{(\pi/2)} \left\{ \frac{gh(\theta_2 - \theta_1)}{\bar{\theta}} \right\}^{1/2} \tag{3}$$

where θ_1 and θ_2 are the potential temperatures at the bottom and top of the stable layer of mean potential temperature $\bar{\theta}$ and h is the depth of the stable layer, we compute a phase speed in the duct, c_{duct}, of 34.9 m s^{-1}. (On the basis of Fig. 10 we chose $\theta_1 = 6$°C, $\theta_2 = 36$°C, $\bar{\theta} = 21$°C and $h = 3$ km.) The observed wave is propagating toward 115° at 18 m s^{-1} at 0000 UTC. Inspection of Fig. 10 reveals that the average wind velocity in the inversion layer is from 170° at 25 m s^{-1}. Thus, our computed phase velocity from (3) *relative to the ground* would be 20.6 m s^{-1}. [As a check, given the possibility of wave contamination of the WAL sounding, a similar calculation for the 1200 UTC 27 February AHN sounding (Fig. 8) yields a value of c_{duct} of 36.6 m s^{-1} where θ_1, θ_2, $\bar{\theta}$ and h are 5°, 35°, 20°C and 3.3 km, respectively. With an average wind velocity of 160° at 30 m s^{-1} below the inversion at AHN and a wave propagation toward 105° at 16 m s^{-1}, a wave speed relative to the ground of 17.2 m s^{-1} is obtained.] The computed phase speed exceeds the observed phase speed by 15%, similar to that found by Bosart and Sanders (1986), who attributed some of the difference to the omission of a moist N in (3) and slight wave supercriticality for nonlinear solitary type waves as described by Christie et al. (1978). Overall, however, the Lindzen and Tung (1976) ducted gravity wave model seems to predict a phase speed similar to the observed.

Comparison of the surface sectional maps (Fig. 12) with the soundings (Figs. 8, 9 and 11) and upper air maps (Fig. 4) for 1200 UTC 27 February reveals that the gravity wave intensifies rapidly in a large-scale environment in which the along-wave thermal wind component is much greater than the cross-wave thermal wind component. Kerry Emanuel (1987, personal communication) has suggested that, under conditions when the component of the thermal wind normal to the gravity wave approaches zero, the existence of a deep layer of symmetric neutrality above the wave duct would favor the trapping of a free gravity wave in the vertical. He has further suggested that the existence of a layer of symmetric instability above the wave duct might favor wave resonance and rapid wave amplification provided the computed and observed wave phase speeds are in good agreement.

Emanuel (1983a,b) showed that symmetric instability was possible in flows for which

$$\frac{\eta}{f} \text{Ri} < 1. \tag{4}$$

That is, symmetric instability can occur in flows characterized by small absolute vorticity, large vertical wind shear and small static stability. Equation (4) was evaluated on the 1° latitude–longitude grid mesh with 100 mb vertical resolution described previously. The Richardson number was computed as the vector shear over 100 mb thick layers. The vorticity was averaged over adjacent 100 mb layers, and the mean value multiplied by the Richardson number to yield (η/f) Ri. A cross section of (η/f) Ri along 35°N for 1200 UTC 27 February given in Fig. 29 shows a sloping region of symmetric instability between 800 and 500 mb from 85° to 80°W across the Appalachian Mountains. The

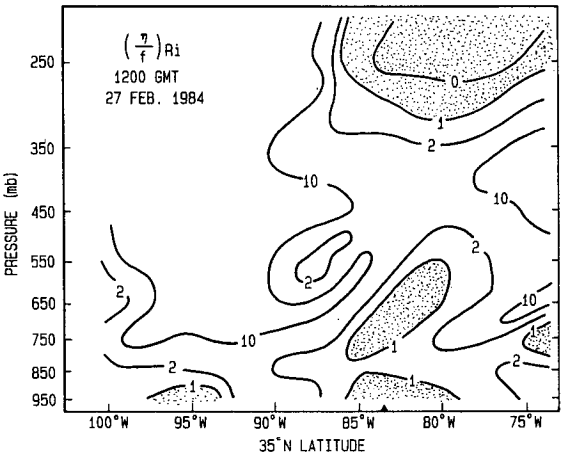

FIG. 29. Cross section of (η/f) Ri along 35°N for 1200 UTC 27 February 1984. Contour intervals of 0, 1, 2 and 10 with stippling for values ≤1.

southern gravity wave (solid triangle) amplifies abruptly near the western *edge* of the symmetrically unstable zone and beneath a region of deep but weak symmetric stability capped by another layer of symmetric instability at jet stream level. By 0000 UTC 28 February (not shown), the intense gravity wave is embedded in areas of symmetric instability below 850 mb, near 600 mb and at the jet stream level. Given the good agreement between the observed and computed wave phase speed from (3), the possibility that wave resonance may have occurred is worthy of debate.

Figures 27b, d show the 0000 UTC 28 February 300 mb and 200 mb divergence field, selected ageostrophic wind vectors and isotachs. At 300 mb (recall Fig. 4c) there is an 80 m s^{-1} jet maximum located over northwestern Georgia so that the gravity wave lies on the anticyclonic shear side of the jet in a diffluent jet exit region. Meanwhile, at 200 mb the strongest jet (subtropical) is centered over western Pennsylvania with a right jet entrance region over eastern North Carolina and Virginia. These conditions ensure the continuation of a favorable environment aloft for the existence of gravity–inertia waves in that large values of divergence are found in regions of appreciable anticyclonic shear and small static stability. The large anticyclonic gyre at 200 mb in the ageostrophic wind field along the North Carolina coast, in conjunction with a ratio of divergence to relative vorticity between 0.5 and 1.0 (Figs. 26c, d), is further evidence that geostrophic adjustment mechanisms can still operate.

c. *Forecasting considerations*

Gravity waves of this amplitude can represent a serious hazard to aircraft operations. The extremely gusty surface winds can be a manifestation of severe turbulence above the ground. Figure 30 shows the location and time of all available pilot turbulence reports for the 12 h ending at 0000 UTC 28 February. Most of these reports came from aircraft flying between 850 and 700 mb. Several pilots remarked that they were unable to maintain altitude in the face of 500 m updrafts and downdrafts or, in a couple of extreme cases, that they were returning to the airport. There are three clusters of activity in Fig. 30. The southernmost smattering of reports comes from aircraft encountering the squall line. The relatively few reports in this region is more attributable to pilot astuteness in avoiding the area than the lack of turbulence. A second clustering occurs in eastern Tennessee and southern Kentucky in the vicinity of 1200 UTC. Here the likely mechanism is the gusty downslope easterly winds as the subsynoptic-scale isallobaric fall center and embedded northern gravity wave moved up west of the mountains and the cross-mountain pressure gradient tightened. The third cluster is located in central North Carolina and southern Virginia. It is centered near 2000 UTC near the

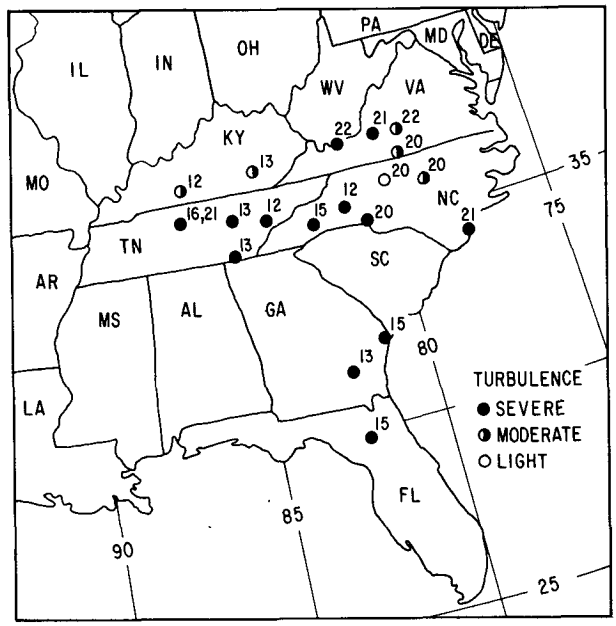

FIG. 30. Reported aircraft turbulence 1200 UTC 27 February–0000 UTC 28 February 1984 with ●, ◑ and ○ denoting severe, moderate and light turbulence, respectively. All times are UTC.

time of maximum wave amplitude. Given the observed weather conditions that day, it is remarkable that there were no serious aircraft mishaps due to unforeseen turbulence.

It is of some interest to examine the then operational Limited Fine Mesh (LFM) model forecast, given the extensive nature of this gravity wave event. Figure 31 shows the 0000 UTC 28 February LFM analysis and verifying 24 h forecast of mean layer relative humidity, the surface cyclone and 500 mb vorticity maxima locations and the 540 dam 1000–500 mb thickness contour. The most noticeable difference between the analysis and the forecast is the LFM failure to capture the observed drying that sweeps across the southeastern United States with the exception of southern Florida. The discrepancy cannot be attributed to a simple phase error. Rather, the model fails to predict the extensive dry slot to the south and east of the cyclone center in the Tennessee and Ohio valleys. Likewise, the error does not arise from the underprediction of cyclogenesis. If anything the LFM 24 h forecast is slightly deeper with the observed low center. We speculate that the extensive region of dry air over the southeastern United States perhaps may be a reflection of the cloud thinning and desiccation and widespread termination of precipitation in the wake of the long-lived gravity wave. Numerical experiments to test this speculation might be of interest, mindful of the disparity in wave scales permitted by the model and the observations.

The propagation of the large amplitude gravity wave and its attendant abrupt weather changes had an impact

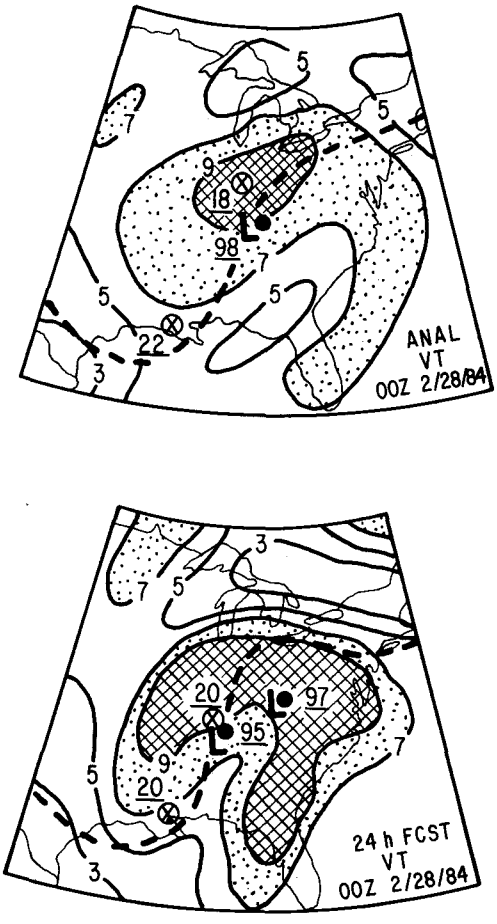

FIG. 31. LFM analysis (top) and 24 h forecast (bottom) valid at 0000 UTC 28 February 1984 of mean relative humidity in the lower half of the troposphere (% × 10, solid); 540 dam 1000–500 mb thickness contour (dashed); 500 mb absolute vorticity centers (⊗ with value × 10^{-5} s^{-1} adjacent); and sea level cyclone (*L* symbol and central pressure, mb, adjacent). Stippling denotes $RH \geq 70\%$.

on NWS operations. For example the Raleigh-Durham NWS office quickly recognized the aforementioned relationship between the damaging surface winds, rapid pressure oscillations and precipitation intensity. They issued several special weather statements in which they advised the public on where and when to expect dramatic weather changes during the afternoon of 27 February. It was an excellent exercise in nowcasting.

At the same time, the extremely large pressure falls in advance of the gravity wave resulted in NMC analyzing a secondary cyclone center near ORF at 0000 UTC 28 February based upon the observed three-hour pressure fall of 12.9 mb (Fig. 12i). As a result, several NWS offices in the Middle Atlantic States issued predictions that the "developing coastal low" was going to become the main storm and move northward toward New England with heavy snow inland. In reality, the cyclone center west of the Appalachians continued as the main storm and considerably warmer air than forecast swept up the Atlantic seaboard.

8. Concluding remarks

Shortly after 0300 UTC 27 February 1984 minor gravity wave activity began in western Tennessee and extreme northern Mississippi in the wake of a slowly intensifying north–south oriented squall line moving eastward across the southeastern United States. Between 0300 and 1200 UTC the wave moved eastward on a heading of roughly 100° at ~15 m s^{-1}. It remained mostly disorganized with pressure oscillations of ~ ±1–2 mb. Surface winds gusted to 10–15 m s^{-1} and precipitation slackened or ended with wave passage. The wave was manifest as a trailing wake depression behind the squall line bubble high in the sea-level pressure field. Beginning around 0900 UTC the trailing wake depression elongated north and south as it approached the Appalachians. The eventual dominant gravity wave continued to organize slowly as the southern lobe approached the Appalachians prior to 1200 UTC. The northern lobe became associated with a separate fall center moving northeastward west of the Appalachians. A fast-moving (~30 m s^{-1}) gravity wave emerged out of this fall area by 1300 UTC in southeastern Kentucky.

Rapid wave intensification was observed between 1200 and 1500 UTC as the southern wave ascended and crossed the southern Appalachians, still on a heading of 100° at ~15 m s^{-1}. The onset of rapid wave amplification coincided closely with the time of peak intensity of the northern portion of the squall line preceding the wave. From the Appalachians eastward to the coast a classic wave of depression was observed. Many stations reported pressure falls of 10 mb or more between wave crest and wave trough. The peak observed wave-induced pressure plunge was 14 mb in 30 minutes at Raleigh-Durham around 2100 UTC. It was accompanied by easterly wind gusts approaching 30 m s^{-1} and the abrupt termination of heavy rain. This association between the pressure changes, the wind changes, and the behavior of the precipitation agrees with the conceptual models of gravity waves given by Eom (1975) and Bosart and Sanders (1986). As the gravity wave approached and crossed the coast it rotated slightly toward a 115° track and accelerated to 20 m s^{-1} after 0000 UTC 28 February. The characteristic wavelength was ~100–150 km with a period of 2–3 h. The locus of maximum pressure drop from wave crest to wave trough showed a clear orographic signature in that it was oriented parallel to the mountains along the Carolina Piedmont region.

Another swath of gusty southeasterly winds could be tracked northeastward in response to a tightened cross Appalachian Mountain pressure gradient associated with the northern wave. This wave moved rapidly away from the stronger southern gravity wave and

after 2100 UTC could no longer be followed in the data across New York and New England.

Both gravity waves formed and amplified in a stable lower troposphere north of a surface frontal boundary and ahead of a jet streak aloft propagating toward a downstream ridge axis. These large-scale environmental features were found to characterize the majority of large amplitude gravity waves reported by Uccellini and Koch (1987). The wave of interest emerged out of a packet of minor pressure oscillations of $\sim \pm 1$–2 mb in the wake of a bubble high to the rear of a slowly intensifying squall line. Geostrophic adjustment was the probable trigger for wave genesis and organization in an upper tropospheric environment in which the divergent and rotational components of the wind had a comparable magnitude of $\sim 10 \times 10^{-5}$ s^{-1}. Shearing instability was ruled out as a likely wave source on the basis of observed wave formation almost parallel to the thermal wind and the absence of a critical level containing sufficient vertical wind shear to produce a Richardson number of $\sim$0.25.

Rapid wave amplification around 1200 UTC 27 February occurred in an environment favorable for geostrophic adjustment. The wave was located in the right exit region of a 35 m s^{-1} low-level southeasterly jet, the right exit region of a 70 m s^{-1} 300 mb jet streak and the right entrance region of a downstream 70 m s^{-1} 200 mb jet streak. Shearing instability at this time, however, could not be ruled out as a wave generation and amplification mechanism because of the increased vertical wind shears associated with the low- and upper-level jets as well as an upstream upper-level frontal zone.

The squall line leading the gravity wave was embedded in a highly baroclinic surface environment. At the northern end of the squall line, the convective elements had their roots in a jet plume of warm, moist unstable air that was being rapidly advected northward above a layer of cool, stable air in the boundary layer. The gravity wave was contained in a trailing wake depression behind the squall line bubble high. This unique relationship was maintained from the time of wave origin to the onset of rapid wave intensification when the convective elements in the northern portion of the line were most vigorous. Branick et al. (1988) have reported a similar association between pressure and wind changes behind an organized mesoscale convective system in the same geographical location.

Compensating subsidence to the rear of the active convective elements in the baroclinic northern portion of the squall line (the so-called wake low effect after Fujita 1959) may have contributed to gravity wave organization and intensification through forced adiabatic subsidence warming and surface pressure reduction in a deep, cold, stable boundary layer. Sufficient hydrostatic warming could be generated by 10 cm s^{-1} subsidence rates to produce surface pressure falls of $\sim$9 mb (20 min)$^{-1}$ in a narrow band behind the squall line, a value close to the observed wave-induced pressure tendency at many locations from the Appalachians eastward.

The wave, once formed, maintained its intensity from the mountains to the coast in the presence of a cold boundary layer capped by a strong stable layer or wave duct. Rapid wave decay was observed after the wave crossed a coastal front boundary that resulted in the removal of the wave duct. The observed behavior of the wave was in very good agreement with the Lindzen and Tung (1976) ducted gravity wave model. The existence of a deep layer of near neutral symmetric stability with embedded layers of symmetric instability above the wave duct may have helped to contribute to wave trapping and wave amplification through a resonance phenomenon involving wave overreflection according to Kerry Emanuel (1987, personal communication).

The northern wave, unlike the southern wave, was manifest as a region of enhanced pressure falls of $\sim$4–7 mb over a 1–2 h period superposed on a prominent lee trough west of the Appalachian mountains in a region of downslope southeasterly flow. The rapid northeastward motion of the wave ($\sim$30 m s^{-1}) was consistent with the upstream presence of a critical layer containing a shear layer in which the Richardson number approached the 0.25 limit for shearing instability. Shearing instability seemed a more likely physical mechanism for wave genesis and organization in this case because the wave fronts were oriented nearly normal to the thermal wind vector through a deep layer of the atmosphere, a condition more favorable for wave trapping in the presence of a critical layer embedded in a strong shear layer. Geostrophic adjustment processes, however, may have played a limited role in the wave evolution given its initial formation just north of the amplifying southern wave. Observations consistent with the possibility of mountain wave-induced lee troughing included the tightening of the cross-mountain pressure gradient in the presence of a mountain top stable layer and the generation of a pocket of clearing skies and warm surface temperatures from eastern Tennessee northeastward to southern West Virginia in an otherwise broad region of cloudy skies.

Finally, the remarkable gravity wave event of 27 February 1984 could serve as a useful testbed for numerical experiments on the degree to which the formation and persistence of intense gravity waves depends upon the configuration of the synoptic-scale flow and the resulting feedback and interaction with mesoscale circulations. For example, evidence was presented which showed that widespread observed cloud thinning and desiccation behind the large-amplitude gravity wave was not replicated in the operational numerical prediction forecasts of mean relative humidity in the lower half of the troposphere.

Acknowledgments. We gratefully acknowledge stimulating conversations about gravity waves with Howie Bluestein, Kerry Emanuel, Dan Keyser, Alan Thorpe and Lou Uccellini. Chris O'Handley provided very helpful computational support. Special thanks are directed to Dave Barber and Jerry Watson of North Carolina State University and Bob Muller of the NWSFO in Raleigh–Durham, North Carolina, for providing us with many critical data items. A thorough, constructive critique by an anonymous referee helped to improve the clarity of the final text. The text was prepared by Celeste Iovinella, and Marilyn Peacock drafted the figures. This research was supported by NSF Grant ATM-8311106.

REFERENCES

Blumen, W., 1972: Geostrophic adjustment. *Rev. Geophys. Space Phys.*, **10,** 485–528.

Bosart, L. F., and J. P. Cussen, Jr., 1973: Gravity wave phenomena accompanying East Coast cyclogenesis. *Mon. Wea. Rev.*, **101,** 446–454.

——, and F. Sanders, 1986: Mesoscale structure in the megalopolitan snowstorm of 11–12 February 1983. Part III: A large-amplitude gravity wave. *J. Atmos. Sci.*, **43,** 924–939.

Branick, M. L., F. Vitale, C.-C. Lai and L. F. Bosart, 1988: The synoptic and subsynoptic structure of a long-lived severe convective system. *Mon. Wea. Rev.*, **116,** 1335–1370.

Brunk, I., 1949: The pressure pulsation of 11 April 1944. *J. Meteor.*, **6,** 181–187.

Christie, D. R., K. J. Muirhead and A. L. Hales, 1978: On solitary waves in the atmosphere. *J. Atmos. Sci.*, **35,** 805–825.

Einaudi, F., W. L. Clark, D. Fua, J. L. Green and T. E. VanZandt, 1987: Gravity waves and convection in Colorado during July 1983. *J. Atmos. Sci.*, **44,** 1534–1553.

Emanuel, K. A., 1983a: On assessing local conditional symmetric instability from atmospheric soundings. *Mon. Wea. Rev.*, **111,** 2016–2033.

——, 1983b: The Lagrangian parcel dynamics of moist symmetric instability. *J. Atmos. Sci.*, **40,** 2368–2376.

Eom, J., 1975: Analysis of the internal gravity wave occurrence of April 19, 1970 in the Midwest. *Mon. Wea. Rev.*, **103,** 217–226.

Ferguson, H. L., 1967: Mathematical and synoptic aspects of a small-scale wave disturbance over the lower Great Lakes area. *J. Appl. Meteor.*, **6,** 523–529.

Fujita, T., 1959: Precipitation and cold air production in mesoscale thunderstorm systems. *J. Meteor.*, **16,** 454–466.

Gossard, E. E., and W. H. Hooke, 1975: *Waves in the Atmosphere. Developments in Atmospheric Science, II.* Elsevier Scientific, 456 pp.

Hoxit, L. R., C. F. Chappell and J. M. Fritsch, 1976: Formation of mesolows or pressure troughs in advance of cumulonimbus clouds. *Mon. Wea. Rev.*, **104,** 1419–1428.

Koch, S. E., and R. E. Golus, 1985: Observed interactions between strong convection and internal gravity waves. *Preprints, 14th Conf. on Severe Local Storms,* Indianapolis, Amer. Meteor. Soc., 198–201.

Ley, B. E., and W. R. Peltier, 1978: Wave generation and frontal collapse. *J. Atmos. Sci.*, **35,** 3–17.

Lin, Y.-H., and R. C. Goff, 1987: A study of a thunderstorm-generated mesoscale solitary wave in the atmosphere. *J. Atmos. Sci.*, **44,** in press.

Lindzen, R. S., and K. K. Tung, 1976: Banded convective activity and ducted gravity waves. *Mon. Wea. Rev.*, **104,** 12, 1602–1617.

Matsumoto, S., and H. Okamura, 1985: The internal gravity wave observed in the typhoon T8124 (Gay). *J. Meteor. Soc. Japan,* **63,** 37–51.

——, K. Ninomiya and T. Akiyama, 1967a: A synoptic and dynamic study on the three-dimensional structure of mesoscale disturbances observed in the vicinity of a cold vortex center. *J. Meteor. Soc. Japan,* **45,** 64–81.

——, —— and ——, 1967b: Cumulus activities in relation to the mesoscale convergence field. *J. Meteor. Soc. Japan,* **45,** 292–304.

Miller, D. G., and F. Sanders, 1980: Mesoscale conditions for the severe convection of 3 April 1974 in the east-central United States. *J. Atmos. Sci.*, **37,** 1041–1055.

O'Handley, C. O., and L. F. Bosart, 1989: Subsynoptic-scale structure in a major synoptic-scale cyclone. *Mon. Wea. Rev.*, **117,** in press.

Pecnick, M. J., and J. A. Young, 1984: Mechanics of a strong subsynoptic gravity wave deduced from satellite and surface observations. *J. Atmos. Sci.*, **41,** 1850–1862.

Pothecary, I. J. W., 1954: Short-period variations in surface pressure and wind. *Quart. J. Roy. Meteor. Soc.*, **80,** 395–401.

Stobie, J. G., F. Einaudi and L. W. Uccellini, 1983: A case study of gravity waves–convective storm interaction: 9 May 1979. *J. Atmos. Sci.*, **40,** 2804–2830.

Uccellini, L. W., 1975: A case study of apparent gravity wave initiation of severe convective storms. *Mon. Wea. Rev.*, **103,** 497–513.

——, and S. E. Koch, 1987: The synoptic setting and possible energy sources for mesoscale wave disturbances. *Mon. Wea. Rev.*, **115,** 721–729.

Van Tuyl, A. H., and J. A. Young, 1982: Numerical simulation of nonlinear jet streak adjustment. *Mon. Wea. Rev.*, **110,** 2038–2054.

Wagner, A. J., 1962: Gravity wave in New England, April 12, 1961. *Mon. Wea. Rev.*, **90,** 431–436.